

**ICE CRYSTAL NUMBER CONCENTRATION
VERSUS TEMPERATURE FOR CLIMATE STUDIES**

*I. Gultepe¹, G. A. Isaac, and S. G. Cober
Meteorological Service of Canada, Toronto,
Ontario, M3H 5T4, Canada*

Accepted

Inter. J. of Climatology

Jan. 31, 2000

¹ *Corresponding author address: I. Gultepe, MSC, Cloud Physics Research Division, Toronto,*

Ontario M3H 5T4, Canada; e-mail: Ismail.gultepe@ec.gc.ca

ABSTRACT

Ice crystal number concentration (N_i) is an important parameter, having a strong influence on the calculation of cloud optical and microphysical parameters. Cloud and precipitation parameterizations within climate and weather forecasting models, affecting the heat and moisture budget of the atmosphere, cannot be determined accurately if N_i is not estimated correctly. Previous studies of ice crystal number concentration versus temperature (T) have shown that N_i -T relationships are not unique. The present study uses observations made in the glaciated regions of stratiform clouds from two Arctic and two mid-latitude field projects to study the N_i versus temperature relationship. Scatter plots of N_i versus T at the ice particle measurement level do not show a good correlation with T for ice crystals at sizes less than 1000 μm . For a given temperature, the variation in N_i is found to be up to 2-3 orders of magnitude for ice crystals with sizes larger than approximately 100 μm . A significant N_i -T relationship is found for precipitation sized particles with sizes greater than 1000 μm . The ice particle concentration for sizes between 100 and 1000 μm varied from 0.1 and 100 l^{-1} , independent of geographic locations where the measurements were made. Based on this work, it is concluded that modeling studies should be tested for the possible variations in N_i versus T.

1.INTRODUCTION

Ice crystal number concentration (N_i) is an important parameter for studying climate change and the general circulation of the atmosphere. It may affect precipitation amount, radiative fluxes, and the heat and moisture budget of the earth's atmosphere (Ghan et al., 1997; Donner et al., 1997). Often, the N_i in general circulation models (GCM) and meso-scale models is initially assumed to be constant or to increase with decreasing temperature (T), and it is also used as a function of supersaturation with respect to ice (S_i). Prognostic equations used in models commonly assume a simple relationship between N_i and T (or S_i) as given in Meyers et al. (1992), Levkov et al. (1995), and Molders et al. (1994). Most of the relationships use the Fletcher curve that is based on the summary of assorted measurements of ice nuclei concentration versus temperature (Fletcher, 1962). Meyers et al. (1992) stated that if the Fletcher formulation is extrapolated to temperatures below those for which it is valid ($\sim -25^\circ\text{C}$), an over-prediction of ice crystal number concentration may occur.

The radiative budget of earth's atmosphere based on an assumed uncertainty in N_i has been studied by some earlier studies. As shown by Gultepe et al. (1998), a 50% uncertainty in equivalent radius (r_{eq}) of an ice crystal may cause a 10 W m^{-2} change in net radiative cloud forcing. Using a prognostic scheme for microphysics in a National Center for Atmospheric Research (NCAR) Community Climate Model (CCM2), Ghan et al. (1997) stated that changing $N_i=100 \text{ m}^{-3}$ to 1000 m^{-3} resulted in the short wave cloud forcing (SWCF) changing from -44.5 W m^{-2} to -31.9 W m^{-2} . Longwave cloud forcing (LWCF) changed from 21.7 W m^{-2} ($N_i=1000 \text{ m}^{-3}$) to 27.3 W m^{-2} ($N_i=100 \text{ m}^{-3}$). Net cloud forcing (NCF) changed from -17.2 W m^{-2} ($N_i=100 \text{ m}^{-3}$) to -10.2 W m^{-2} ($N_i=1000 \text{ m}^{-3}$). These results also showed that a one order of magnitude

change in N_i could result in a 70% change in net radiative cloud forcing. This indicates that a one order of magnitude uncertainty in ice crystal concentration, which certainly exists in the measurements reported in this paper, may significantly affect the heat budget of the atmosphere.

Climate modeling studies using ice microphysics have been performed by Senior and Mitchell (1993), Fowler and Randall (1996a; 1996b) and Lohmann et al (2001). It is shown by Senior and Mitchell (1993) that the CO_2 doubling effect was reduced when constant cloud optical properties were replaced by the variable ones as a function cloud ice and water paths. Fowler et al. (1996a; 1996b) used the Colorado State University GCM to study the impact of liquid and ice microphysics and interactive cloud optical properties on the cloudiness, the earth radiation budget, and cloud radiative forcing. Using various ice microphysical parameterization schemes, they found that uncertainties related to ice microphysics resulted in a net cloud forcing approximately between -26 W m^{-2} and -43 W m^{-2} . Lohmann et al (2001) showed that there were poor comparisons between a single column model results and some of the observations used in the present study. These studies also indicated that ice crystal number concentration is the important parameter for better understanding atmospheric heat and moisture budget.

Ice crystal nucleation processes can be divided into 5 different types: 1) Deposition (sublimation), 2) Contact, 3) Condensation-freezing, 4) Bulk freezing (immersion-freezing), and 5) Homogeneous nucleation. Types 2 and 4 need a pre-existing droplet for nucleation. Homogeneous nucleation occurs when T is less than -40°C (Fletcher, 1962) where an insoluble nucleus is necessary for ice crystal formation. Definitions of the processes can be found in Isaac and Douglas (1972), Pruppacher and Klett (1980), and Dennis (1980). These processes were

generally studied using cloud chambers where T was held constant. In the atmosphere, these modes cannot be separated easily. Ice multiplication (Hallet and Mossop, 1974) is assumed not to occur in the cloud chamber, although this assumption may be incorrect. In such studies, ice particle concentrations (N_i) measurements are assumed as predictors of IN (for symbols see Appendix) concentrations and so IN concentrations are often referred to as N_i .

Aufm Kampe and Weickmann (1957) summarized the results relating N_i to T from Palmer (1949), Aufm Kampe and Weickmann (1951), Smith and Heffernan (1954), and Workman and Reynolds (1949). They found that the variability in N_i for a given T was about 5 orders of magnitude at -15°C . Based on similar earlier studies, Fletcher (1962) showed that the relationship determined from the observations of ice nuclei number concentration and T is usually exponential, resulting in a straight line in the $\log N_i$ - T plot over the temperature range -10 to -30°C (Fig. 1).

Using cloud chambers and laboratory measurements, Huffman and Vali (1973) and Huffman (1973a,b) derived relationships between N_i and T , and N_i and S_i . The results were found to be significantly different than earlier studies. A large variability in N_i for a given T indicated that N_i might depend on thermodynamical, dynamical, and aerosol characteristics (DeMott et al., 1994). It is also possible that differences in the N_i measured in the laboratories can be attributed to the performance and mode of operation of ice nuclei counters.

Al-Naimi and Saunders (1985), Cooper (1980), and Deshler (1982) collected data from aircraft and cloud chambers to study N_i versus T and S_i . In general, their observations were

representative of the environment between -2 and -20°C . These studies showed that N_i did not show a good correlation with T . Using earlier studies, Meyers et al. (1992) showed that ice crystal concentration values were directly related to S_i . Earlier observations were limited due to a lack of observations in some environmental conditions such as $T < -25^{\circ}\text{C}$ where no relationship was suggested to estimate N_i from T . Rogers et al. (1996) and Rogers and Vali (1987) used aircraft data to study the N_i - T relationship within a wave cloud. The study of their works indicated a spread of the N_i over almost the entire range of observations at $T < -10^{\circ}\text{C}$. This was likely due to IN and S_i variability in the atmosphere. The relationship suggested by Sassen (1992) differed from Fletcher curve by a height dependent exponential term. This was done to account for the expected lower concentrations of ice nuclei (aerosol) at high altitudes. Heymsfield and Milosheovich (1993) reported on several instances of low numbers of IN at high altitudes at $T < -25^{\circ}\text{C}$. Rogers et al. (1998) and DeMott et al. (1998) confirmed that IN concentrations can be as much as two orders of magnitude lower than values given by the typical “Fletcher curve” at temperatures around -30°C . At cold temperatures ($< -45^{\circ}\text{C}$), based on earlier studies, Jensen and Toon (1994) stated that ice crystal number concentrations were usually only a small fraction of the total number of aerosols present ($N_i \sim 1\text{-}300 \text{ l}^{-1}$ versus aerosol number concentration, $N_a, \sim 10\text{-}500 \text{ cm}^{-3}$). Brientjes et al. (1994) used a relationship that simply assumed N_i as a constant for temperatures less than -20°C . Collectively, these studies show that N_i characteristics, especially at cold temperatures ($< -20^{\circ}\text{C}$) in the atmosphere, need to be studied in detail.

Ryan (1996) pointed out that N_i from some parameterized equations are much lower than those obtained from in-situ observations. Conversely, N_i values have been found to be lower than

parameterized equations such as the Fletcher curve (Rangno and Hobbs, 1994; Hobbs and Rangno, 1985). In fact, ice enhancement or ice multiplication is defined as a phenomenon when ice crystal number concentrations are significantly higher than those expected from the Fletcher curve (Hobbs, 1969; Rangno and Hobbs, 1991). Ice multiplication processes (Hallet and Mossop, 1974; Rangno and Hobbs, 1994; Hobbs and Rangno, 1985), aggregation (Gorden and Marwitz, 1984; Marwitz, 1987; Mitchell, 1988), and fall-out from the clouds (Heymsfield and Donner, 1990; Donner et al., 1997), which depend on environmental conditions, can have significant influence on N_i -T relationships.

Vertical air velocity (w_a) is an important parameter used in the study of ice crystal number concentration. Blyth and Latham (1993) used aircraft observations obtained from summertime cumulus clouds with continental origin. They found that increasing w_a likely results in a low N_i value due to a high liquid water content (LWC) and the collision/aggregation process, whereas N_i was significantly larger when w_a was less than $+3 \text{ m s}^{-1}$. However, a model study of cirrus cloud (DeMott et al., 1994) showed that maximum N_i in a lifting air parcel increases with increasing w_a . These results indicate that dynamical processes are still not fully understood.

In-situ observations of N_i and T, collected within stratiform clouds from four field projects that took place over the Arctic region and mid-latitudes, are used in the present work. The objective of this work is to study the N_i -T relationship over three size ranges including 1) less than $100 \mu\text{m}$, 2) greater than $100 \mu\text{m}$, and 3) greater than $1000 \mu\text{m}$, for Arctic ice clouds and mid-latitude frontal clouds, particularly with respect to their use for climate and cloud studies. The importance of aerosol, dynamical and thermodynamical parameters on the N_i -T relationship

will also be examined. This work differs from other investigations, because the observations cover the T range from 0°C to -45°C, and include measurements from three very different geographical regions. Earlier studies, including the in-situ and cloud chamber measurements, were primarily in the T range of -2 to -30°C. Also, most of the earlier studies did not consider the averaging scale as an important parameter, and this factor is considered in this paper.

The observations section provides detailed information on the in-situ measurements. The analysis of in-situ observations for the four field projects is described in the method section. In the results section, relationships and variability obtained from the in-situ observations of the present study are summarized. Finally, a discussion of the results, including comparisons with earlier studies, and conclusions related to climate studies are given.

2.OBSERVATIONS

In-situ observations from four field projects are used in this study. The Beaufort and Arctic Storms Experiment (BASE) and the Canadian participation in the First ISCCP (International Satellite Cloud Climatology Project) Regional Experiment-Arctic Cloud Experiment (FIRE.ACE) that took place over the Arctic region (Northwest Territories) of Canada during the fall of 1994 and the spring of 1998 (Gultepe et al., 2000a; 2000b; Curry et al., 2000), respectively. The Canadian Freezing Drizzle Experiment (CFDE) I took place over Eastern Canada (mainly offshore) during the winter of 1994-1995 and CFDE III was conducted in Ontario during the winter of 1997-1998.. The details on these two projects can be found in Isaac et al. (1998). A National Research Council Convair-580 was the aircraft used for all projects.

Cloud systems during BASE originated from both the Arctic and Pacific Oceans (Gultepe et al, 2000a) and the observations were primarily made in frontal clouds. Although the main goal of FIRE.ACE was to collect measurements in boundary layer clouds, the Convair-580 often flew above the boundary layer. Consequently, some cloud types (cirrus, altostratus, altocumulus, stratus, and stratocumulus) were examined covering a temperature range from 0°C to -45°C. The purpose of CFDE I and III was to study aircraft icing related microphysical characteristics of winter storms. These clouds were primarily stratiform associated with warm frontal regions.

The T measurements used in this study were obtained from both Rosemount and reverse-flow temperature probes with an uncertainty of $\pm 1.0^\circ\text{C}$. The Particle Measuring Systems (PMS) forward scattering probes (model FSSP-100) were set up for size ranges of 5-95 μm (called FSSP-124) and 2-47 μm (called FSSP-096). The PMS two-dimensional cloud (2D-C) and precipitation (2D-P) probes were used to estimate N_i for size intervals of 25-800 μm and 200-6400 μm , respectively.

The FSSP is designed to measure droplet characteristics although it does respond significantly to ice particles. Details and uncertainties related to the FSSP measurements can be found in Baumgardner et al. (1985; 1990). Gardiner and Hallett (1985) showed that false counts due to ice particles could be as high as 2-3 orders of magnitude greater than the actual ice crystal number concentration, although they were only able to explain a factor of approximately 30. Gayet et al. (1993; 1996) suggested that, in the presence of large non-circular ice crystals with sizes greater than 1000 μm , the FSSP could overestimate ice particle concentration by about one order of magnitude. Arnott et al. (2000) showed that FSSP and 2D-C measurements within

cirrus overlap decently when the large particle concentration is low enough (it is about $0.1-1.0 \text{ l}^{-1}$ for the present work). In their work, FSSP N_i for a tropical cirrus was a factor of 2 less than 2D-C N_i for sizes $< 50 \mu\text{m}$. They found that a large discontinuity at the FSSP and 2D-C overlap region is present when there are large and irregular ice particles, and they stated that the source of the exaggerated response of the FSSP to ice particles is not clear. The effect of the refractive index on sizing for water and ice obtained from FSSP measurements was studied by Gayet et al (1996). They found that its effect on sizing is rather small when particle diameter is larger than $5 \mu\text{m}$, and it can be neglected as opposed to other errors inherent to airborne applications.

The uncertainties in measuring N_i with a 2D-C probe were studied by Vali et al. (1981), Gordon and Marwitz (1984), and Gayet et al. (1993). They discussed undercounting at smaller size channels. Gayet et al stated that PMS 2D-C probes were considered to be accurate only for particles with sizes greater than $50 \mu\text{m}$. They suggested that the determination of the sampling volume may also be a source of uncertainties in N_i , because of its dependency on sampling area, particle size and shape, and duration. They also suggested that the problem of image digitization may affect the sizing and therefore lead to an underestimation of concentrations. In the present study, each 2D hydrometeor image was processed following the center-in technique of Heymsfield and Parrish (1978), and artifacts (out of focus, particles too large, etc.) were filtered out.

In the present study, FSSP probe measurements are qualitatively used as a surrogate for estimating ice crystal number concentration when the particle size is less than $100 \mu\text{m}$. This is only done when clouds with liquid droplets are removed from the data set, as described in the

analysis section. The 2D-C measurements of N_i are used safely in the analysis when the particle size is $\geq 125 \mu\text{m}$. The 2D-P measurements are used for particle sizes $\geq 1000 \mu\text{m}$. Detailed analysis of these observations are given in the next section.

3. ANALYSIS

The Convair-580 instrumentation was similar for the four field projects for which data was analyzed. In each field project, 2D-C, 2D-P, and FSSP probes were mounted on pylons under the wings of the aircraft. The temperature used in the analysis is the temperature at the height where the ice particles were observed, and it may not be related the temperature for actual ice particle formation. The N_i were obtained from the integration of N_i over the PMS 2D-C and 2D-P bins from 125 to 800 μm and 1000 to 6400 μm , respectively, along 30-second ($\sim 3 \text{ km}$) segments. A cloud region was assessed when ten or more hydrometeors were observed during the 30-s averaging interval, as determined from the PMS 2D-C probe.

Glaciated cloud regions were identified following the techniques developed by Cober et al. (2000a). They demonstrated that differences in the instrument responses to ice particles versus water drops could be used to segregate liquid, mixed, and glaciated cloud regions. In addition to a Rosemount icing detector (RID; Cober et al, 2000b), the instruments used in the analysis were a King LWC (Cober et al., 2000b), a Nevzorov LWC/TWC (Korolev et al., 1998), a 2D-C (Gayet et al., 1993), and two FSSP (Baumgardner et al., 1990) probes. By combining the data from several instruments, glaciated cloud regions could be identified with a high level of confidence. Cober et al. (2000b) found that when temperatures $< -4^\circ\text{C}$, the averaged RID signal change per second was $< 2 \text{ mv s}^{-1}$ in 98.5% of the glaciated clouds observed during CFDE I and III. They concluded that using a

threshold of 2 mv s^{-1} would eliminate all LWC clouds with $\text{LWC} > 0.01 \text{ g m}^{-3}$. The sensing element of the RID is an axially vibrating tube whose natural frequency changes as ice accumulates on it. The frequency-to-voltage converter changes the difference frequency to a voltage, and this can be validated against LWC. Clouds with $\text{LWC} < 0.01 \text{ g m}^{-3}$ could not be detected with the RID because at such low LWC values, the mass transfer on the RID sensor from evaporation exceeded that from accretion (Mazin et al. 2000).

The King and Nevzorov LWC probes were found to measure $< 20\%$ of the TWC in glaciated cloud regions (Cober et al. 2000a), with the apparent LWC signal being caused by the instrument responses to ice crystals. For FSSP measurements in mixed and glaciated clouds, ice crystals were found to have a significant effect for sizes $> 35 \text{ }\mu\text{m}$, independent of the instrument or ranges used. This caused the FSSP spectra median volume diameter (MVD) to exceed $30 \text{ }\mu\text{m}$ in all the glaciated clouds identified in CFDE I and III (Cober et al. 2000a). Similarly, no glaciated cloud in CFDE I and III had a FSSP concentration $> 15 \text{ cm}^{-3}$. Finally, Cober et al. (2000a) showed that the frequency occurrence of irregular shaped crystals with sizes $\geq 125 \text{ }\mu\text{m}$ in diameter in glaciated clouds was always > 0.6 , while that of circular particles was always < 0.4 . Circular particles were identified using diameter, area, perimeter, and symmetry ratios, that compared the idealized circular area of an ice crystal to that of a real ice crystal image.

While none of these criteria are individually able to fully segregate glaciated and non-glaciated clouds, the combination of these criteria can be used to identify glaciated cloud segments with a high degree of confidence. Cober et al. (2000a) suggested that an averaged RID rate $< 2 \text{ mv s}^{-1}$, FSSP MVD $> 30 \text{ }\mu\text{m}$, the ratio of Nevzorov LWC to TWC < 0.2 , the ratio of the number of circular particles to the number of non-circular particles < 0.4 , and FSSP concentration $< 15 \text{ cm}^{-3}$

could be used to assess glaciated cloud conditions. Only clouds with trace amounts ($< 0.01 \text{ g m}^{-3}$) of LWC would fail to be identified with this methodology. They also argued that a trace amount of LWC in the presence of ice crystals would be rapidly evaporated, so that clouds with trace amounts of LWC were unlikely to be included in the identified subset of glaciated clouds.

N_i observations for PMS 2D-C 50-100 Φm size intervals are used for comparisons with the FSSP based number concentrations (N_{if}). Arnott et al. (2000) and Gayet et al. (1996) suggested that FSSP measurements in glaciated conditions can be used for N_i measurements. It was shown that FSSP spectra reasonably agreed with the spectra of the Desert Research Institute Cloud Scope Instrument when the concentration of large particles was low enough (Arnott et al., 2000). The accuracy of the N_{if} values also depends on how precisely cloudy regions that contain liquid water drops can be removed from the data set using the technique described above. It should be cautioned that the apparent large number of small ice crystals makes it difficult to obtain accurate total ice crystal number concentrations. Just quoting PMS 2D-C concentrations, although they give reasonable estimates for particles larger than 125 Φm , would be misleading if N_i at small sizes were not considered. Perhaps, when newer instruments such as the SPEC Inc. (Boulder, CO) Cloud Particle Imager (CPI) (Lawson et al., 2000) can accurately measure the concentration of smaller particles, this problem can be overcome.

4.RESULTS

Results obtained from the analysis of in-situ observations related to N_i and T are given in this section.

4.1 Summary of Observations

Ice particle number concentrations from each probe (see Observations section) obtained along constant altitude flight legs and vertical profiles, representing 30-s averages (3 km path length), are averaged at 2°C intervals, and then used in the analysis. The N_i from the 2D-C probe for $L_i \geq 125 \mu\text{m}$ will be represented as N_{idu} , N_i for $L_i < 125 \mu\text{m}$ will be represented as N_{idl} . Table 1 shows mean values of N_{idu} and the number of data points used at each T interval for each project. Biases in the field projects can be seen based on the number of data points. For example, FIRE.ACE contains statistically significant data covering -10 to -45°C while CFDE I contains significant data over the range of 0 to -14°C.

Figs. 2a to 2d for the BASE observations are obtained for N_{idu} ($L_i \geq 125 \mu\text{m}$), N_{idl} ($L_i < 125 \mu\text{m}$), N_{ip} ($L_i \geq 1000 \mu\text{m}$), and the ice crystal number concentration from the FSSP probe (5-95 μm), N_{if} ($L_i < 100 \mu\text{m}$), respectively. The selection of the cutoff threshold diameter strongly affects N_i . Similarly, Figs. 3a to 3d, 4a to 4d, and 5a to 5d are obtained for FIRE.ACE, CFDE I, and CFDE III, respectively. Problems related to depth of field calculations causes large uncertainties in the N_{idl} measurements. The lines from right to the left for each figure shows the frequency of occurrence of N_i averaged at 2°C intervals for 100%, 90%, 75%, 50%, 25%, and 10%, respectively. The dark solid line is for the mean values. It should be re-emphasized that the values of N_{idu} and N_{ip} can be estimated accurately (approximately a factor of 2), while N_{idl} and N_{if} contain the significant uncertainties discussed in the previous section. Note that the number of points (N_p) at cold temperatures is less than at warm temperatures (Table 1) and this may cause greater uncertainty at cold temperatures.

The most important result is that for N_{idu} , N_{idl} , N_{ip} , and N_{if} there is a large spread in values, approximately up to three orders of magnitude at each temperature interval. This tends to obscure any trends, except perhaps for N_{ip} that will be discussed further. .

Summaries of the mean N_i from all probes for the four projects are shown in Figs. 6 to 9, respectively. It is seen that N_{ip} (as 2D-P measurements) gradually increases for colder T from 0°C to -13°C for all projects except for CFDE III where its values were approximately constant. While below -13°C , N_{ip} can include large uncertainties due to variability in the measurements, it tends to decrease with decreasing T . N_{idl} and N_{idu} are almost constant up to -30°C , and then start to fluctuate. These fluctuations may be due to the limited number of data points used in the averaging at cold temperatures. In general, N_{if} from both FSSPs are constant within one order of magnitude with large fluctuations at low T . N_{if} is approximately 2-3 order of magnitude greater than N_{idu} .

4.2 Comparisons

In this section, the results are compared to earlier parameterizations of N_i or IN versus T . The 30-s averages of N_{idu} from the PMS 2D-C probe for all projects and the curves representing earlier parameterizations (Table 2) are shown in Fig. 10. Note that Eq. 6 given in Table 2 is obtained using a best fit to N_i and T observations of Rogers et al. (1996) collected within wave clouds. The mean values of N_{idu} for all projects, averaged over 2°C intervals, have been plotted over the entire temperature range of the measurements.. It should be noted that N_{idu} are usually less than 100 l^{-1} . Although the relationships of Table 2 were meant to show the variability of ice nucleus concentrations with temperature or supersaturation, they have often been used to

predict ice particle concentrations. Consequently, the ice nucleus versus temperature relationships are plotted against the observations from this study. It is clear that the data do not follow any of the parameterizations shown in Fig. 10.

Comparisons of N_{ip} from all projects are shown in Fig. 11. The line labeled CCB represents the averaged observations for stratiform clouds with some precipitation from CFDE I and III, and BASE that were related to synoptic scale processes. The FIRE.ACE line represents cold stratiform cloud systems with a negligible precipitation, and in general they are not related large-scale processes. In this figure, N_{ip} gradually increases with decreasing T at warm T 's for all projects excluding CFDE III, while at colder temperatures (below -13°C) the concentration decreases significantly. As noted before, because of a large variability (standard deviation) in the mean values, the relationships should be used cautiously. The increase in N_{ip} near -13°C may be explained by the increase in growth rates at this temperature, due to a large saturated vapor pressure difference over ice and water. The decrease in N_{ip} at temperatures colder than -13°C is probably caused by a lack of water vapor that restricts the growth of large ice particles in a low supersaturation environment. These results are verified using particle size, shape, and concentration analysis at various supersaturations observed during the Canadian field projects. The relationships between N_{ip} and T are given in Table 3. The large correlation coefficient (R) value indicates that there is a strong correlation between N_{ip} and T . It should be noted that fall-out of large ice particles (size $>1000\ \mu\text{m}$) in precipitating clouds may have some effects on profiles for individual clouds.

4.3 Variability in N_i measurements

The variability in the measurements of N_i can be very large based on the environmental conditions at various S_i , T , vertical air velocity, and IN concentrations. The values of N_i at lower sizes ($<100 \mu\text{m}$) cannot be obtained accurately with the 2D-C probe (Gordon and Marwitz, 1984; Gayet et al., 1993 and 1996; Arnott et al., 1994). In order to estimate uncertainties in the measurements, we performed two tests: 1) N_{idl} is compared with N_{idu} , and 2) N_{idl} is compared with N_{if} (FSSP-100 concentration).

The results related to both tests are given in Table 4. The N_{if} , N_{idl} , N_{idu} are given in columns 2, 3, and 4, respectively. Column 5 shows the ratio of N_{if} to N_{idu} . This ratio is about 2-3 orders of magnitude, implying that that N_{idu} accounts for only 0.1 to 1% of the N_i . Note that because of an uncertainty of about 2-3 order of magnitude in N_{if} , one should be careful for quantifying the uncertainty in 2D-C measurements. In the last column, N_{idl}/N_{idu} , is approximately 51%. It is understood that the 2D-C concentrations for sizes less than or equal to $100 \mu\text{m}$ are poor because of the large uncertainty in sample volume, and that the FSSP concentration in the presence of ice crystals may be significantly flawed because of multiple counting. These measurements were summarized in order to gain a first order approximation of concentrations and the variation with temperatures. It is expected that the 2D-C N_i for particle sizes less than $100 \mu\text{m}$ is underestimated while the FSSP N_i is overestimated. In addition, the errors are expected to be systematic (Fig. 6) so that the concentration variation with T should still be relevant.

5.DISCUSSION

The large variability in N_i in earlier studies was likely caused by several effects including a fixed temperature in the cloud chambers, the limited number of data points, different averaging

intervals or sample volumes, and the lack of in-situ observations. In general, the data collected prior to 1970 was obtained at a relative humidity saturated with respect to water and at temperatures between -30°C and -5°C . It should be noted that uncertainties at both ends of the curve fit (i.e. temperatures $>-10^{\circ}\text{C}$ and $<-25^{\circ}\text{C}$) are likely larger than the values in the center (see Fig. 1). This is likely caused by the inhomogeneous distribution of data points. The parameterized equation for ice nuclei concentration versus T suggested by Fletcher was obtained primarily from ground based observations. Aufm Kampe and Weickmann (1957) showed similar observations, but did not attempt to obtain a parameterization that shows increasing N_i with decreasing T .

Ryan (2000) obtained N_i from a limited area model (Katzfey and Ryan, 1997) and compared it to N_i observed within cirrus and frontal clouds during observational studies. His model results, using the Heymsfield and Platt (1984) parameterization, showed that N_i at the frontal cloud tops decreased from about 80 l^{-1} (-17°C) to $2-3 \text{ l}^{-1}$ (-47°C). Overall, his model results were found comparable to the observations except that the observed ice crystal number concentration exceeded the diagnosed N_i between -22.5°C and -27.5°C . These results showed that the N_i versus T relationship is still not known in detail because these results do not agree with earlier studies in which N_i increases with decreasing T .

Recent studies have primarily used optical array probes within cloud and cloud chambers to examine the relationship between N_i and T . Many of the previous studies were in fact not representative of various environmental conditions (e.g. T , relative humidity, and velocity field)

and cloud types. Conversely, in-situ observations in the present study were collected under numerous environmental conditions over a large T interval range ($>0^{\circ}\text{C}$ and $<-45^{\circ}\text{C}$).

A large uncertainty in the data may occur as a result of the analysis or averaging method used. For example, clear air regions used in the averaging intervals can significantly lower the mean values. Gultepe and Isaac (1999) discussed the effect of space scales on droplet concentrations, and similar conclusions would likely be reached for ice particle concentrations. In an analysis of measurements made off the Canadian East Coast, Isaac (1991) showed that ice particle concentrations could change depending on the averaging interval. The selection of averaging interval of 30 s (approximately 3 km) used in the present study minimizes the effects of clear air regions.

It is clear that the N_i -T relationship depends on the size threshold used for N_i . At larger sizes ($>1000\ \mu\text{m}$), a relationship appears to exist at temperatures less than -13°C (Fig. 11). It should be clarified that each curve in Fig. 11 represent unique environmental conditions, and averaging of all the data including its variability should be used carefully when model comparisons are made. At smaller ice crystal sizes, no obvious relationship exists between N_i and T (Figs. 3 to 5). Small ice crystals can exist in very large concentrations, although they are difficult to measure. The small ice particles measured by the CPI probe during FIRE.ACE did not suggest seeding from above. Overall, seeding from the high level clouds was not a dominant process for the field project data used in the present study. Details on the CPI for N_i measurements can be found in Lawson et al (2000).

It could be argued that one should use the cloud top temperature or the coldest in-cloud temperature to determine the relationship between N_i and T , as done by Hobbs and Rangno (1998). However, the largest concentrations are clearly seen at the smallest sizes ($<100 \text{ }\mu\text{m}$). These particles can grow quickly, and they must have been generated near the measurement level. Consequently, when using in-situ measurements to obtain N_i versus T relationships, it would seem that the temperature at the measurement level is a suitable temperature for use in the analysis. This is also verified using Table 4 where N_{if} is at least two order of magnitude greater than $N_{id>125 \text{ }\mu\text{m}}$. This result should be used carefully when the accuracy of FSSP measurements are in suspect.

Some examples from the 17 April case of FIRE.ACE are given in Fig. 12 to indicate the importance of w_a , RH_i , and N_a in the calculation of N_i . This figure likely reflects equilibrium conditions after the nucleation processes. In this case, measurements with the equilibrium RH_i may not be the same as those that existed when the ice crystals formed. The w_a was obtained using a Rosemount 858 5-hole pressure probe and Litton LTN-90-100 Inertial Reference System. The rms error for w_a is about 0.15 m s^{-1} (MacPherson, 1993). Relative humidity with respect to ice (RH_i) was obtained from a LiCor Hygrometer. The T_d measurements from this probe can be more reliable at cold temperatures (Gultepe et al., 2000c) as compared to the EG&G Hygrometer dewpoint measurements. Interstitial aerosol number concentrations (N_{ai}) were obtained from a PMS passive cavity aerosol spectrometer probe (PCASP-100X) sampling in 15 channels in the range of $0.12\text{-}3 \text{ }\mu\text{m}$. N_i was obtained from 1Hz 2D-C total particle-counts for all channels.

Fig. 12a shows N_i versus N_{ai} . It is clear that there is no linear relationship between them. When N_{ai} increases larger than 100 cm^{-3} , N_i decreases. The ability of an ice formation process to limit nucleation due to water vapor competition and reduction in supersaturation, and thus affect the relationship to aerosols at low temperatures is well known (Heymsfield and Sabin, 1989; Jensen and Toon, 1994). Considering ice formation in a parcel of air, N_i versus N_{ai} can be limited by ice crystal growth to produce a distribution such as that shown in Fig. 12a. Fig. 12b shows N_i versus RH_i , which also is related to supersaturation. This plot shows that the maximum N_i increases with increasing RH_i up to $RH_i=120\%$, and then it decreases with increasing RH_i . The N_i versus RH_i relationship is not clear and likely requires more detailed studies. Fig. 12c shows that the smaller absolute values of w_a at the equilibrium conditions result in large N_i values. This can be explained by the lack of collision/aggregation processes when w_a is small. In this figure, the mean w_a is taken out of the observations collected over the constant altitude flight legs at about -10°C over a thirty-minute time period. In stratiform clouds, it has been suggested that an increase in w_a within an air parcel results in increasing N_i (Findeisen and Schulz, 1944; DeMott et al., 1994), but this figure indicates that this is not always true. For $\sim 35\%$ of the time in the Arctic stratus clouds on 17 April, a larger w_a resulted in lower N_i . This characteristic should also be considered in the parameterization of N_i .

Gultepe et al (2000b) suggested a relationship based on a heat budget equation for climate change studies, and this relationship shows that w_a and RH_i are important for determining N_i in modeling studies. It should be noted that N_i versus T within wave clouds can be significantly different than these of stratiform clouds. For example, the study of Rogers et al. (1996) showed that N_i in such clouds increases slightly with decreasing T . This could likely be due to well-

defined dynamical and thermodynamical processes within the wave clouds. Results from Fig. 12 indicate that a detailed analysis among N_i , N_{ai} , RH_i , and w_a under the equilibrium environmental conditions is needed for a better understanding of climate change-cloud interactions.

Although there are many uncertainties related to the Fletcher curve, his relationship has been used extensively in the literature. The following works are given as examples. The number of ice crystals nucleated by the deposition-freezing mode, including height effects, was given by Sassen (1992) as

$$N_i(T) = A_{so} \exp(-A_z z) \exp[B_s(T_s)], \quad (1)$$

where A_{so} is the measured value of ice nuclei (IN) at the earth's surface which is $1 \times 10^{-5} \text{ l}^{-1}$. A_z is 0.75 at altitude z , and $B_s(T_s)$ is the same as in Fletcher (1962). At cold temperatures such as $T < -20^\circ\text{C}$, the Fletcher curve can result in a large uncertainty because it is derived from a high T range. N_i values shown in Fig. 10 indicate that N_i at colder temperatures for the present study can be highly variable compared to those that would extrapolated from the Fletcher curve. Other modeling studies, including Levkov et al. (1995), Harrington et al. (1995), Molders et al. (1994), also used Fletcher curve extensively for meso-scale modeling. For ice clouds representing mostly cirrus, Heymsfield and Platt (1984) suggested a parameterization for the particle size spectrum in terms of ambient temperature, ice water content, and ice crystal maximum dimension. This parameterization indicated that it may be better to use such a relationship for other cloud types.

6. CONCLUSIONS

The N_i values from the present study are found to be comparable to those of previous studies. In fact, although the four projects reported in this study were conducted at different times and for at least 3 different locations, the ice particle concentrations scattered all over the T ranges were similar, being between 0.1 and 100 l^{-1} . No strong relationship was found between N_i and T when the ice crystal size is less than $1000 \mu\text{m}$, and N_i is found to be highly variable (Fig. 10). This indicates that if the variability is not included, parameterizations used in modeling studies may lead to large uncertainties in microphysical parameters and related derived parameters. In contrast to the small ice particles, the N_{ip} decreases with decreasing T ($< -13^\circ\text{C}$) for precipitation size particles ($> 1000 \mu\text{m}$) with a correlation coefficient of $\sim 0.50-0.93$. It would be useful to study N_i versus aerosol number concentration and T at various ice and water saturated regions of the clouds. Then, comparisons with the climate and meso-scale models could be improved.

Small ice particles appear to dominate the ice particle concentration. It is unlikely that these particles could have formed at higher levels and been brought down in downdrafts without sublimating completely. If they formed below and rose to the current level in an updraft, they would grow to much larger sizes. It seems reasonable to assume they were formed at or near the temperature at the measurement level. This justifies the procedure used in this paper of relating N_i to the temperature at the ice particle measurement level. However, it is unclear why such large concentrations of small ice particles exist.

The number concentration of ice crystals with sizes less than $100 \mu\text{m}$, as estimated from the FSSP probes, indicated that N_{if} could be as high as 1.5 to 3 orders of magnitude higher than N_{idu} . The problems associated with accurate measurements of the concentration of small ice

crystals are many. However, the concentration at small sizes must be known before an accurate relationship between N_i and T can be obtained.

In the current analysis, the 30-s or approximately 3-km averaging scale was used in the calculations. It should be noted that increased time and space scales result in less scatter or variability. Therefore, the parameterizations developed need to be specified based on the time and space scales used or required for the application.

The results from the present study suggest that the earlier parameterizations should be used with caution in climate studies, and that, if possible, vertical air velocity, supersaturation with respect to ice, and aerosol number concentration should be included in the N_i parameterizations. This conclusion agrees with a study of cold cirrus clouds by Heymsfield and Sabin (1989) who stated that the number of ice crystals produced is a function of the temperature, vertical air velocity, and the ice nuclei (IN) concentration.

Beyond the possible dependencies on vertical air velocity and supersaturation mentioned above, there are many factors which can affect the N_i - T relationship including, nucleation, ice multiplication, aggregation and ice particle growth rates. Each of these factors probably has a different relationship with temperature, although it would be difficult to quantify them in any precise manner. Since the aerosol number concentration tends to decrease with altitude and the temperature also decreases with altitude, this could partially explain the observations. Although, Fig. 12a indicates no strong relationship between aerosol concentration and N_i , this needs further study, perhaps using an aerosol surface area as the dependent variable. Ice

multiplication mechanisms, other than that proposed by Hallett and Mossop (1974), which only apply at warm temperatures, might also be responsible for uncertainties. For example, evaporating ice crystals might splinter into many small particles resulting in a large number of crystals at smaller sizes. Such small ice crystals, in a presence of saturated air with respect to ice, would grow out of the small size range. Only continuous ice multiplication or continued nucleation of new crystals could easily explain the observed size distributions. It is likely that in a controlled environment, N_i versus other parameters could be studied to better understand how ice particle forms and develops.

Acknowledgments: The authors are thankful to reviewers for their constructive comments that improved this manuscript, significantly.

The Panel on Energy Research and Development provided financial support for BASE and FIRE.ACE. Additional support was given from NASA for the collection of the FIRE.ACE data. The National Search and Rescue Secretariat of Canada, Boeing Commercial Airplane Group, Transport Canada, and the Department of National Defense provided funding for the CFDE projects. The aircraft data were obtained using the National Research Council of Canada Convair-580 and the scientific and technical efforts of many National Research Council (NRC) and Meteorological Service of Canada (MSC) staff. The authors thank W. Strapp of MSC for discussions related to data analysis. Data extraction from the 2D-C and 2D-P measurements was based on software developed by A. V. Korolev and S. G. Cober. Authors also thank B. Baker and P. Lawson of SPEC Inc., Boulder, CO, as well as A.V., Korolev, for discussions related to CPI observations of small particle concentrations.

Appendix:***Symbols used in the present study***

IN: Ice nuclei.

L_i : Ice crystal size.

LWC: Liquid water content

N_a : Aerosol number concentration.

N_i : Ice crystal number concentration from any probe.

N_{ai} : Interstitial aerosol number concentration

N_{id} : Ice crystal number concentration from 2D-C probe (25-800 μm).

N_{idl} : Ice crystal number concentration from 2D-C probe when an ice crystal size (L_i) < 125 μm .

N_{idu} : Ice crystal number concentration from 2D-C probe when an ice crystal size (L_i) \geq 125 μm .

N_{if} : Ice crystal number concentration from FSSP-100 probes (5-95 μm for FSSP-124 and 2-47 μm for FSSP-096).

N_{imax} : Maximum ice crystal number concentration from any probe.

N_{ip} : Ice crystal number concentration from 2D-P probe (200-6400 μm).

N_{IN} : Ice nuclei number concentration.

RH_i : Relative humidity with respect to ice.

S_i : Supersaturation with respect to ice.

T: Temperature.

TWC: Total water content

w_a : Vertical air velocity.

REFERENCES

Al-Naimi, R., and C. P. R. Saunders, 1985: Measurements of natural deposition and condensation-freezing ice-nuclei with a continuous-flow chamber. *Atmos. Environ.*, **19**, 1871-1882.

Arnott, W. P., Y. Dong, J. Hallett, and M. R. Poellot, 1994: Role of small ice crystals in radiative properties of cirrus: A case study, FIRE II, 22 November 1991. *J. Geophys. Res.*, **99**, 1371-1381.

Arnott, W. P., D. Mitchell, C. Schmitt, D. Kingsmill, and D. Ivanova, 2000: Analysis of the FSSP performance for measurement of small crystal spectra in cirrus. 13th International Conference on Clouds and Precipitation, 14-18 August 2000, Reno, Nevada. Accepted.

Aufm Kampe, H. J., and Weickmann, H. K., 1951: The effectiveness of natural and artificial aerosols as freezing nuclei. *J. Meteor.*, **8**, 283.

Aufm Kampe, H. J., and H. K. Weickmann, 1957: Physics of clouds, **v. 3, No. 18**, chapter in *Meteorological Monographs* edited by A. K. Blackadar, 182-225.

Baumgardner, D., J. W. Strapp, and J. E. Dye, 1985: Evaluation of the forward scattering spectrometer probe. II: Corrections for coincidence and dead-time losses. *J. Atmos. Ocean. Tech.*, **2**, 626-632.

Baumgardner, D., W. A. Cooper, and J. E. Dye, 1990: Optical and electronic limitations of the forward scattering spectrometer probe, *Liquid Particle Size Measurements Techniques: 2nd Volume*, ASTM STP 1083, E. Dan Hirleman, W. D. Bachalo, and P. G. Felton, Eds., American Society for Testing and Materials. Philadelphia, 115-127 pp.

Blyth, A. M., and J. Latham, 1993: Development of ice and precipitation in New Mexican summer time cumulus clouds. *Q. J. R. Meteor. Soc.*, **119**, 91-120.

Bruintjes, R. T., T. L. Clark, and W. D. Hall, 1994: Interactions between topographic airflow and cloud/precipitation development during the passage of a winter storm in Arizona. *J. Atmos. Sci.*, **51**, 48-67.

Cober, S.G., G.A. Isaac, A.V. Korolev, and J.W. Strapp, 2000a: Assessing mixed phase conditions. *J. Appl. Meteor.*, *accepted*.

Cober, S.G., G.A. Isaac, and A.V. Korolev, 2000b: Assessing the Rosemount icing detector with in-situ measurements. *J. Atmos. Oceanic Technol.*, *submitted*.

Cooper, W. A., 1980: A method of detecting contact ice nuclei using filter samples. Preprints, *Eighth International Conf. on Cloud Physics*, Clermont-Ferrand, France, 665-668.

Cotton, W. R., G. J. Tripoli, R. M. Rauber, and E. A. Mulvihill, 1986: Numerical simulation of the effects of varying ice crystal nucleation rates and aggregation processes on orographic snowfall. *J. Clim. Appl. Meteor.*, **25**, 1658-1680.

Curry, J. A., P.V Hobbs, M. D. King, D.A. Randall, P. Minnis, G.A. Isaac, J.O. Pinto, T. Uttal, A. Bucholtz, D.G. Cripe, H. Gerber, C.W. Fairall, T.J. Garrett, J. Hudson, J.M. Intrieri, C. Jakob, T. Jensen, P. Lawson, D. Marcotte, L. Nguyen, P. Pilewskie, A. Rangno, D. Rodgers, K.B. Strawbridge, F.P.J. Valero, A.G. Williams, and D. Wylie, 2000: FIRE Arctic clouds experiment. *Bull. Amer. Meteor. Soc.*, 81, 5-30.

DeMott, P. J., M. P. Meyers, and W. R. Cotton, 1994: Parameterization and impact of ice initiation processes relevant to numerical model simulations of cirrus clouds. *J. Atmos. Sci.*, **51**, 77-90.

DeMott, P. J., D. C. Rogers, S. M. Kreidenwies, Y. Chen, C. H. Twohy, D. Baumgardner, and A. J. Heymsfield, 1998: The role of heterogenous freezing nucleation in upper tropospheric clouds: Inferences from SUCCESS. *Geophys. Res. Lett.*, **25**, 1387-1390.

Dennis, A. S., 1980: *Weather Modification by Cloud Seeding*. Academic Press, New York, 267 pp.

Deshler, T., 1982: *Contact ice nucleation by submicron atmospheric aerosols*. Ph.D. Dissertation, Dept. of Physics and Astronomy, University of Wyoming, 107 pp.

Donner, L. J., C. J. Seman, B. J. Soden, R. S. Hemler, and J. C. Warren, 1997: Large-scale ice clouds in the GFDL SKYHI general circulation model. *J. Geophys. Res.*, **102**, D18, 21745-21768.

Fletcher, N. H., 1962: *Physics of Rain Clouds*. Cambridge University Press, 386 pp.

Findeisen, W. and G. Schulz, 1944: Experimentelle Untersuchungen über die atmosphärische Eisteilchenbildung. I. *Forsch.-u. ErfahrBer. Reichsamt Wetterdienst A*, 27 pp.

Fowler, L. D., and D. A. Randall, 1996: Liquid and ice cloud microphysics in the CSU General Circulation Model. Part II. Impact on cloudiness, the Earth's budget and the general circulation of the atmosphere. *J. Climate*, **9**, 530-560.

Fowler, L. D., and D. A. Randall, 1996: Liquid and ice cloud microphysics in the CSU General Circulation Model. Part III. Sensitivity to modeling assumptions. *J. Climate*, **9**, 561-586.

Gardiner, B. A., and J. Hallett, 1985: Degradation of in-cloud forward scattering spectrometer probe measurements in the presence of ice particles. *J. Atmos. Ocean. Tech.*, **2**, 171-180.

Gayet, J.-F., P. A. Brown, and F. Albers, 1993: A comparison of in-cloud measurements obtained with six PMS 2D-C probes. *J. Atmos. Ocean. Tech.*, **10**, 180-194.

Gayet, J. F., G. Febyvre, and H. Larsen, 1996: The reliability of the PMS FSSP in the presence of small ice crystals. *J. Atmos. Ocean. Tech.*, **13**, 1300-1310.

Ghan, S. J., L. R. Leing, and Q. Hu, 1997: Application of cloud microphysics to NCAR community climate models. *J. Geophys. Res.*, **102**, D14, 16507-16527.

Gordon, G. L., and J. D. Marwitz, 1984: An airborne comparison of three PMS probes. *J. Atmos. Ocean. Tech.*, **1**, 22-27.

Gultepe, I., and G. A. Isaac, 1999: Relationship between droplet and aerosol number concentrations from aircraft observations: Applications for climate models. *J. Climate*, **12**, 1268-1279.

Gultepe, I., G. A. Isaac, A. Korolev, S. Cober, and J. W. Strapp, 1998: Effects of ice crystal shape on the radiative characteristics of low level ice clouds. Preprints, *Conference on Cloud Physics*, 17-21 August, Everett, Washington, 372-375.

Gultepe, I., G.A. Isaac, D. Hudak, R. Nissen, and J. W. Strapp, 2000a: Dynamical and microphysical characteristics of Arctic clouds during BASE. *J. Climate*, **13**, 1225-1254.

Gultepe, I., and G. A. Isaac, 2000b: The effects of airmass origin on Arctic cloud microphysical parameters during FIRE.ACE. *J. Geophys. Res.*, submitted.

Gultepe, I., G. A. Isaac, J. I. MacPherson, and K. Strawbridge, 2000c: Characteristics of moisture and heat fluxes over leads and polynyas, and their effects on Arctic cloud microphysics during FIRE.ACE. *J. Geophys. Res.*, , submitted.

Hallet, J., and S. C. Mossop, 1974: Production of secondary ice particles during the riming processes. *Nature*, **249**, 26-28.

Harrington, J. Y., M. P. Meyers, R. L. Walko, and W. R. Cotton, 1995: Parameterization of ice crystal conversion processes due to vapor deposition for mesoscale models using double-moment basis functions. Part I: Basic formulation and parcel model results. *J. Atmos. Sci.*, **52**, 4344-4366.

Heymsfield, A. J., and J. L. Parrish, 1978: A computational technique for increasing the effective sampling volume of the PMS two-dimensional particle size spectrometer. *J. Appl. Meteor.*, **17**, 1566-1572.

Heymsfield, A. J., and C. M. R. Platt, 1984: A parameterization of the particle size spectrum of ice clouds in terms of the ambient temperature and ice water content. *J. Atmos. Sci.* **41**, 846-855.

Heymsfield, A. J., and R. M. Sabin, 1989: Cirrus crystal nucleation by homogenous freezing of solution droplets. *J. Atmos. Sci.*, **46**, 2252-2264.

Heymsfield, A. J., and L. J. Donner, 1990: A scheme for parameterizing ice-cloud water content in general circulation models. *J. Atmos. Sci.*, **47**, 1865–1877.

Heymsfield, A. J., and L. M. Milosovich, 1993: Homogenous ice nucleation and supercooled liquid water in orographic wave clouds. *J. Atmos. Sci.*, **50**, 2335-2353.

Hobbs, P. V., 1969: Ice multiplication in clouds. *J. Atmos. Sci.*, **26**, 367-381.

Hobbs, P. V., and A. L. Rangno, 1985: Ice particle concentrations in clouds. *J. Atmos. Sci.*, **42**, 2523-2549.

Hobbs, P. V., and A. L. Rangno, 1998: Microstructure of low and middle-level clouds over the Beaufort Sea. *Q. J. R. Meteorol. Soc.*, **124**, 2035-2071.

Huffman, P. J., 1973a: *Supersaturation dependence of ice nucleation by deposition for silver iodide and natural aerosols*. Report No. AR 108, available from University of Wyoming, Laramie, Wyoming, 29 pp.

Huffman, P. J., 1973b: Supersaturation spectra of AgI and natural ice nuclei. *J. Appl. Meteor.*, **12**, 1080-1087.

Huffman, P. J., and G. Vali, 1973: The effects of vapor depletion on ice nucleus measurements with membrane filters. *J. Appl. Meteor.*, **12**, 1018-1024.

Isaac, G. A., and R. H. Douglas, 1972: Another “time lag” in the activation of atmospheric ice nuclei. *J. Appl. Meteor.*, **11**, 490-493.

Isaac, G. A., 1991: Microphysical characteristics of Canadian Atlantic storms. *Atmos. Res.*, **26**, 339-360.

Isaac, G.A., S.G. Cober, A.V. Korolev, J.W. Strapp, A. Tremblay, and D.L. Marcotte, 1998: Overview of the Canadian Freezing Drizzle Experiment I, II and III. *Preprints, Cloud Physics Conf.*, Everett, WA., Amer. Meteor. Soc., 447-450.

Jensen, E. J., and O. B. Toon, 1994: Ice nucleation in the upper troposphere: sensitivity to aerosol number density, temperature, and cooling rate. *Geophys. Res. Lett.*, **21**, 2019-2022.

Katzfey, J. J., and B. F. Ryan, 1997: Modification of thermodynamic structure of the lower troposphere by the evaporation of precipitation: A GEWEX cloud study. *Mon. Wea. Rev.*, **125**, 1431-1466.

Korolev, A.V., J.W. Strapp, G.A. Isaac, and A. Nevzorov, 1998: The Nevzorov airborne hot wire LWC/TWC probe: Principles of operation and performance characteristics. *J. Atmos. Ocean. Tech.*, **15**, 1496-1511

Lawson, P. R., B. A. Baker, and C. G. Schmitt, 2000: An overview of microphysical properties of Arctic clouds observed in May and July 1998 during FIRE.ACE. *J. Geophys. Res.*, accepted.

Levkov, L., M. Boin, and B. Rockel, 1995: Impact of primary ice nucleation parameterizations on the formation and maintenance of cirrus. *Atmos. Res.*, **38**, 147-159.

Lohmann, U., J. Humble, W. R. Leitch, G. A. Isaac, and I. Gultepe, 2001: Simulations of ice clouds during FIRE.ACE using the CCCMA single column model. *J. Geophys. Res.*, accepted.

MacPherson, J. I., 1993: Use of a wing-mounted airflow pod for airborne wind and flux measurements. Preprints, Eighth Symp. On Meteorological Observations and Instrumentations, Anaheim, CA, Amer. Meteor. Soc., 169-174.

Marwitz, J.D., 1987: Deep orographic storms over the Sierra Nevada. Part II: The precipitation process. *J. Atmos. Sci.*, **44**, 174-185.

Mazin, I.P., A.V. Korolev, A. Heymsfield, G.A. Isaac and S.G. Cober, 2000: Thermodynamics of icing cylinder for measurements of liquid water content in supercooled cloud. *J. Atmos. Oceanic Tech.*, submitted.

Meyers, M. P., P. J. DeMott, and W. R. Cotton, 1992: New primary ice-nucleation parameterizations in an explicit cloud model. *J. App. Meteor.*, **31**, 708-721

Mitchell, D. L., 1988: Evolution of snow-size spectra in cyclonic storms. Part I: Snow growth by vapor deposition and aggregation. *J. Atmos. Sci.*, **45**, 3431–3451.

Molders, N., H. Hass, H. J. Jakobs, M. Laube, and A. Ebel, 1994: Some effects of different cloud parameterizations in a meso-scale model and a chemistry transport model. *J. Appl. Meteor.*, **33**, 527-545.

Palmer, H. P., 1949: Natural ice-particle nuclei. *Q. J. R. Meteor. Soc.* **75**, 15.

Pruppacher, H. R., and J. D. Klett, 1980: *Microphysics of Clouds and Precipitation*. D. Reidel Publishing Company, Boston, 714 pp.

Rangno, A. L., and P. V. Hobbs, 1991: Ice particle concentrations and precipitation development in small polar maritime cumuliform clouds. *Q. J. R. Meteorol. Soc.* **117**, 207-241.

Rangno, A. L. and P. V. Hobbs, 1994: Ice particle concentrations and precipitation development in small continental cumuliform clouds. *Q. J. R. Meteorol. Soc.*, **120**, 573-601.

Rogers, D. C. and G. Vali, 1987: Ice crystal production by mountain surfaces. *J. Clim. And App. Met.*, **26**, 1152-1168.

Rogers, D. C., P. J. DeMott, W. A. Cooper, and R. M. Rasmussen, 1996: Ice formation in wave clouds: Comparison of aircraft observations with measurements of ice nuclei. *12th Inter. Conf.*

on Clouds and Precipitation Proceedings-V.1, Zurich, Switzerland, 19-23 August, V.1, 135-137.

Rogers, D. C., P. J. DeMott, S. M. Kreidenweis, Y. Chen, 1998: Measurements of ice nucleating aerosols during SUCCESS. *Geophys. Res. Lett.*, **25**, 1383-1386.

Ryan, B. F., 1996: On the global variation of precipitating layer clouds. *Bull. Amer. Meteor. Soc.*, **77**, 53-70.

Ryan, B. F., 2000: A bulk parameterization of the ice particle size distribution and the optical properties in ice clouds. *J. Atmos. Sci.*, **57**, 1436-1451.

Sassen, K., 1992: Ice nuclei availability in the higher troposphere: Implications of a remote sensing cloud phase climatology. *Nucleation and Atmospheric Aerosols*, N. Fukuta and P. Wagner, Eds., Deepak Publishing, 287-290.

Senior, C. A., and J. F. B. Mitchell, 1993: Carbon dioxide and climate: The impact of cloud parameterization. *J. Climate*, **6**, 393-417

Smith, E. J., and K. J. Heffernan, 1954: Airborne measurements of the concentration of natural and artificial freezing nuclei. *Quart. J. R. Met. Soc.*, **80**, 182.

Vali, G., M. K. Politovich, and D. G. Baumgardner, 1981: Conduct of cloud spectra measurements. Air Force Geophysical Laboratories, Rep. No. AFGL-TR-0122, 69 p. [NTIS AD-A102-944/6].

Warner, J., 1957: An instrument for the measurement of freezing nucleus concentration. *Bull. Obs. Puy de Dome*, p.33.

Workman, E. J., and S. E. Reynolds, 1949: Thunderstorm electricity. New Mexico Inst. Min. Tech., Prog. Rep., No. 6.

Young, K. C., 1974: A numerical simulation of wintertime, orographic precipitation: Part I. Description of model microphysics and numerical techniques. *J. Atmos. Sci.*, **31**, 1735-1748.

2DC probe measurements when size $\geq 125 \mu\text{m}$								
T [°C]	BASE		FIRE.ACE		CFDEI		CFDEIII	
	\overline{N}_{idu} [l ⁻¹]	# of points	\overline{N}_{idu} [l ⁻¹]	# of points	\overline{N}_{idu} [l ⁻¹]	# of points	\overline{N}_{idu} [l ⁻¹]	# of points
-46;-44	-	-	0.3	11	-	-	-	-
-44;-42	0.5	14	1.0	133	-	-	-	-
-42;-40	2.0	10	1.8	63	-	-	-	-
-40;-38	5.6	5	4.1	54	-	-	-	-
-38;-36	1.1	3	5.1	125	-	-	-	-
-36;-34	5.7	8	4.3	64	-	-	-	-
-34;-32	3.0	16	5.7	131	-	-	-	-
-32;-30	2.1	145	2.3	133	11.4	20	5.2	34
-30;-28	4.1	388	2.5	121	6.9	38	13.7	35
-28;-26	3.7	134	6.4	70	5.5	44	8.5	41
-26;-24	3.5	63	3.1	107	4.8	12	7.1	46
-24;-22	3.1	75	3.8	66	3.2	49	5.0	56
-22;-20	2.7	152	2.0	109	1.3	83	6.9	138
-20;-18	3.6	111	2.4	213	2.5	52	7.6	137
-18;-16	2.2	58	1.5	178	2.3	51	7.4	247
-16;-14	2.3	64	1.9	96	2.6	33	7.1	250
-14;-12	2.7	97	2.5	62	4.2	139	5.7	360
-12;-10	1.9	153	0.9	109	5.0	88	3.3	383
-10;-8	1.5	137	1.5	32	5.4	117	3.2	382
-8;-6	1.6	269	2.2	29	5.3	359	4.5	570
-6;-4	2.6	248	2.5	24	9.4	312	6.0	523
-4;-2	2.7	189	3.8	2	8.0	366	6.6	472
-2;0	1.6	139	1.0	3	5.8	112	5.1	265

Table 1: Mean values of N_{idu} and number of points used at each T interval for each field project.

Authors	Relationship	T[°C] range	Nucleation type	Parameters Used in Eqs.	R ²	Eq. #
Fletcher (1962)	$N_{id}(dT)=n_o \exp(\beta dT)$	-15;-30	DF	$n_o=10^{-5} \text{ l}^{-1}$, $\beta=0.6^\circ\text{C}^{-1}$	-	1
Huffman (1973a,b)	$N_{id}=[(S_i-1)(S_o-1)^{-1}]^b$	-12;-20	DF	$b=4.5$	-	2
Huffman and Vali (1973)	$N_{id}=N_{do} \exp(bdT)$ $(S_i-1/S_o-1)^\beta$	-12;-20	DF	$N_{do}=10^{-5} \text{ l}^{-1}$, $b=0.6^\circ\text{C}^{-1}$ $\beta=4.5\text{C}^{-1}$	-	3
Cotton et al. (1986)	$N_{id}=N_o[(S_i-1)$ $(S_{io}-1)^{-1}]^b \exp(aT_{sup})$	-10;-20	DF	$N_o=10^{-5} \text{ l}^{-1}$, $a=0.6^\circ\text{C}^{-1}$, $b=4.5$	-	4
Meyers et al. (1992)	$N_{id}=\exp\{a+$ $b[100(S_i-1)]\}$,	-7;-20	DF	$a=-0.639$ $b=0.1296$	0.82	5
Rogers et al. (1996)	$N_{id}=0.0063$ $\exp(-0.281T)$,	-10;-35	DF	T:temperature	-	6
Young (1974)	$N_{ic}=N_{ao}(270.16T_c)^{1.3}$	-3;-20	CF	$N_{ao}=2.0 \times 10^2 \text{ l}^{-1}$ at 0 km to 10 l^{-1} at 5 km	-	7
Meyers et al. (1992)	$N_{ic}=\exp[a+$ $b(273.15-T_c)]$	-2;-20	CF	$a=-2.80$ $b=0.262 \text{ l}^{-1}$	0.52	8

Table 2: Previous parameterizations used by modeling studies. S_o is the supersaturation with respect to ice (S_i) at water saturation. T_c is the cloud temperature. DF and CF are for deposition-condensation freezing nucleation and contact freezing nucleation, respectively. dT is the supercooling rate. R is the correlation coefficient. Note that Eq. 6 representing wave clouds is obtained using a best fit to the N_i versus T observations of Rogers et al. (1996).

Relationship between N_i and T for 2DP measurements when size is greater than 1000 μm .				
Field project	Temperature range [$^{\circ}\text{C}$]	Relationship	Correlation Coefficient (R)	Cloud type
BASE	0 to -13	$N_i=0.20\exp(-0.06T)$	0.60	Arctic precipitating stratiform clouds
BASE	-13 to -35	$N_i=15.70\exp(0.26T)$	0.92	Arctic precipitating Stratiform clouds
FIRE.ACE	0 to -13	$N_i=0.0003\exp(-0.47T)$	0.72	Arctic stratiform clouds
FIRE.ACE	-13 to -45	$N_i=3.29\exp(0.28T)$	0.50	Arctic stratiform clouds
CFDEIII	0 to -13	$N_i=0.46\exp(-0.002T)$	0.70	Mid-latitude precipitating and non-precipitating stratiform clouds
CFDEIII	-13 to -32	$N_i=4.18\exp(0.142T)$	0.93	Mid-latitude precipitating and non-precipitating stratiform clouds
CFDEI	0 to -13	$N_i=0.32\exp(-0.094T)$	0.91	Mid-latitude precipitating and non-precipitating stratiform clouds
CFDEI	-13 to -32	$N_i=301.2\exp(0.446T)$	0.88	Mid-latitude precipitating and non precipitating stratiform clouds
CCB	0 to -13	$N_i=0.32\exp(-0.054T)$	0.85	Precipitating and non-precipitating stratiform clouds
CCB	-13 to -32	$N_i=20.79\exp(0.252T)$	0.93	Precipitating and non-precipitating stratiform clouds

Table 3: Relationships representing best fits for N_{ip} versus T in Fig. 11 for each project. The CCB curve represents a fit for CFDEI, CFDEIII, and BASE observations combined. See text for grouping observations from the field projects.

Uncertainty in N_{id} for size $\geq 125 \mu\text{m}$ for BASE					
T [°C]	N_{if} [I ⁻¹]	$N_{id<125}$ [I ⁻¹]	$N_{id\geq 125}$ [I ⁻¹]	$\frac{N_{if}}{N_{id\geq 125}}$	$\frac{N_{id\geq 125}}{N_{id<125}}$
-46;-44	-	-	-	-	-
-44;-42	138	1.3	0.5	276	0.38
-42;-40	657	5.0	2.0	328	0.40
-40;-38	990	49	5.6	356	0.11
-38;-36	1405	9.7	1.1	425	0.11
-36;-34	2834	34	5.7	497	0.17
-34;-32	1602	10	2.0	801	0.20
-32;-30	1025	2.5	2.1	488	0.84
-30;-28	713	3.9	4.1	174	1.05
-28;-26	1108	4.1	3.7	300	0.90
-26;-24	885	4.0	3.5	253	0.88
-24;-22	2486	3.6	3.1	802	0.86
-22;-20	933	3.2	2.7	346	0.85
-20;-18	896	6.2	3.6	249	0.58
-18;-16	2767	3.8	2.2	1258	0.58
-16;-14	1258	4.4	2.3	547	0.52
-14;-12	1323	5.5	2.7	490	0.49
-12;-10	2402	5.7	1.9	1264	0.33
-10;-8	1449	4.3	1.5	966	0.36
-8;-6	2404	4.4	1.6	1503	0.36
-6;-4	2224	5.8	2.6	855	0.45
-4;-2	2021	7.0	2.7	749	0.39
-2;0	1587	5.1	1.6	992	0.31
Mean	2342	6.3	2.7	867(~%0.1)	%51

Table 4: N_{if} , N_{idl} , N_{idu} , N_{if}/N_{idu} , and N_{idu}/N_{idl} versus T for BASE field project. See text for symbols.

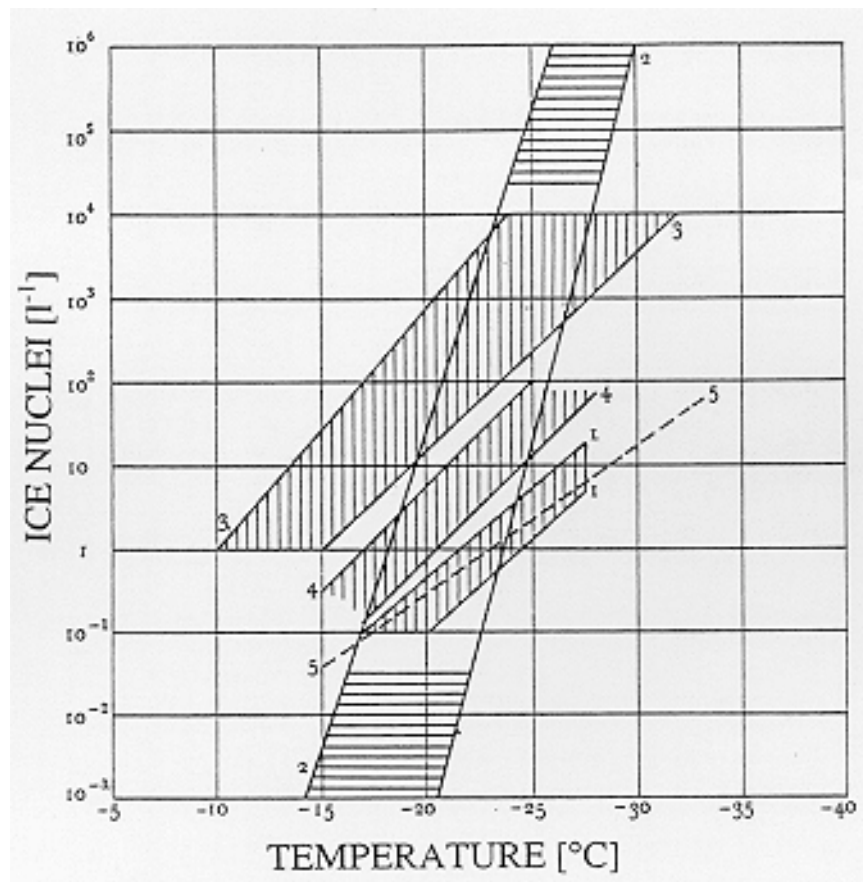


Fig. 1: Natural ice-nucleus spectra versus temperature (Fletcher, 1962). This figure shows observations of Palmer, 1949 (1); Workman and Reynolds, 1949 (2); Aufm Kampe and Weickmann, 1951 (3); thermal precipitator (4); Warner, 1957 (5). The numbers in parenthesis represent the lines in the figure.

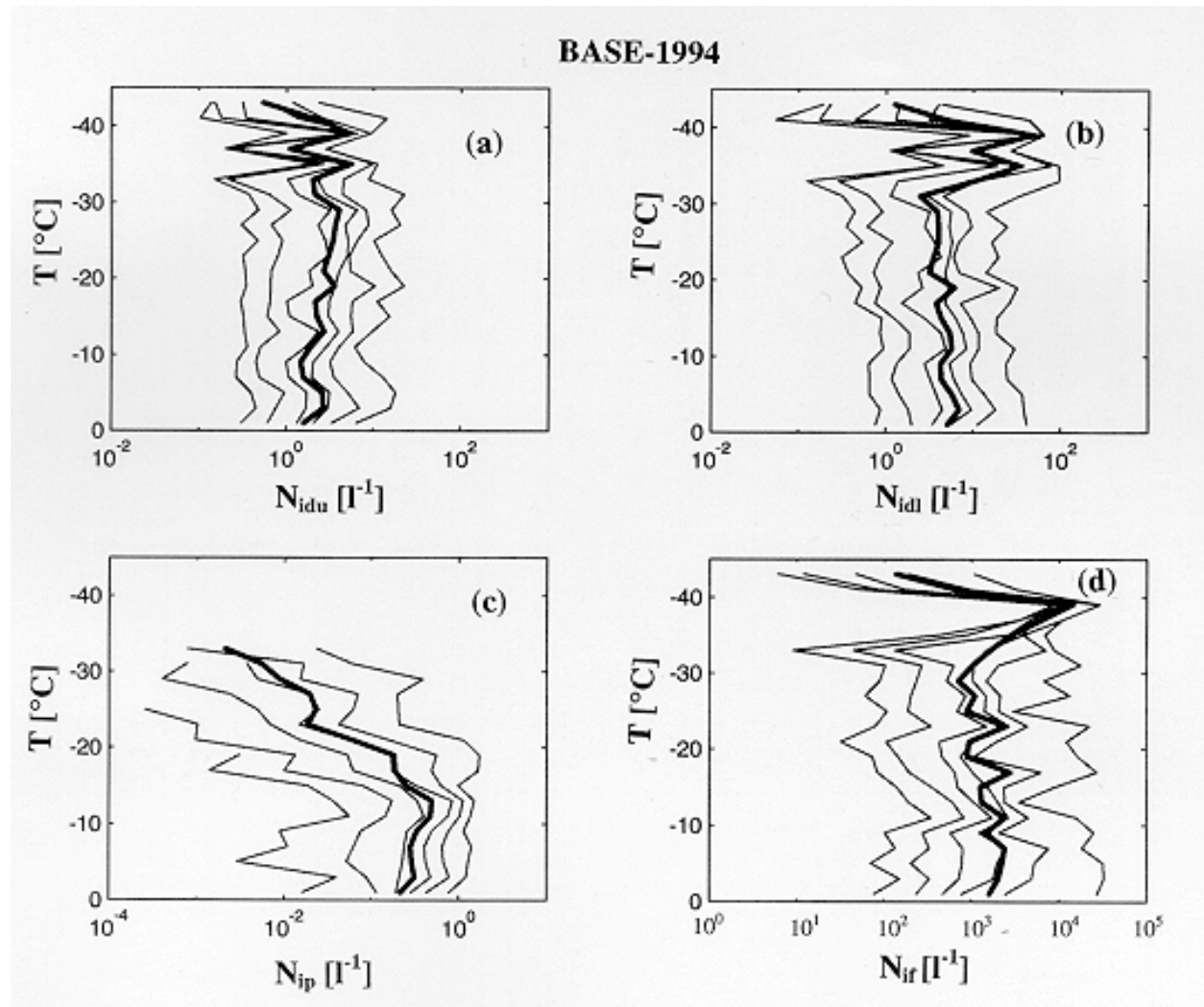


Fig. 2: The N_{idu} , N_{idl} , N_{ip} , and N_{if} (see Appendix) averaged over 2°C intervals at standard conditions are shown in boxes a to d, respectively. See (Appendix) for symbol definitions. The lines from right to the left at each figure represent the frequency occurrence of N_i over 2°C intervals for 100%, 90%, 75%, 50%, 25%, and 10% percentiles, respectively. The dark solid line is for the mean values.

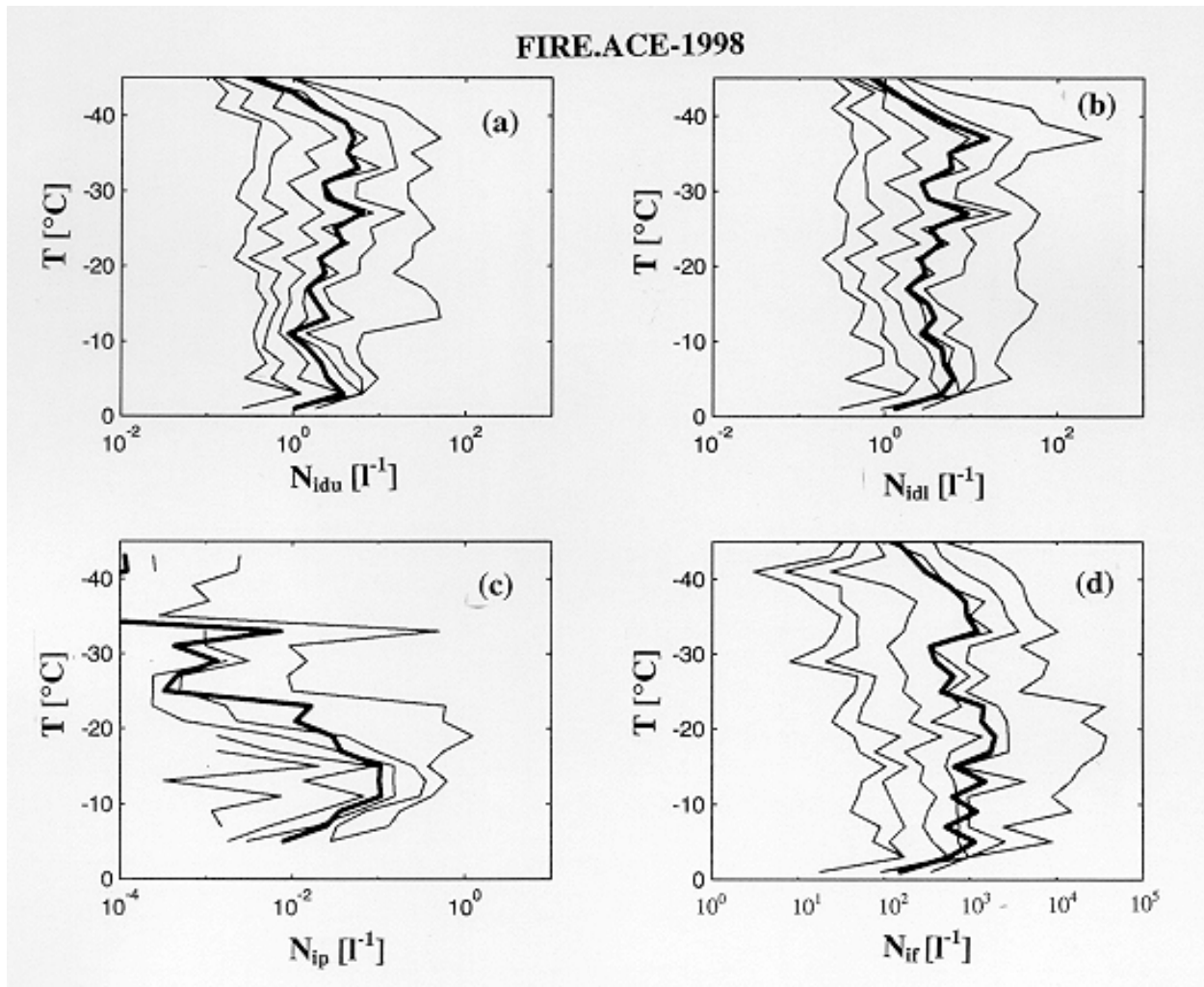


Fig. 3: Same as Fig. 3 except for FIRE.ACE.

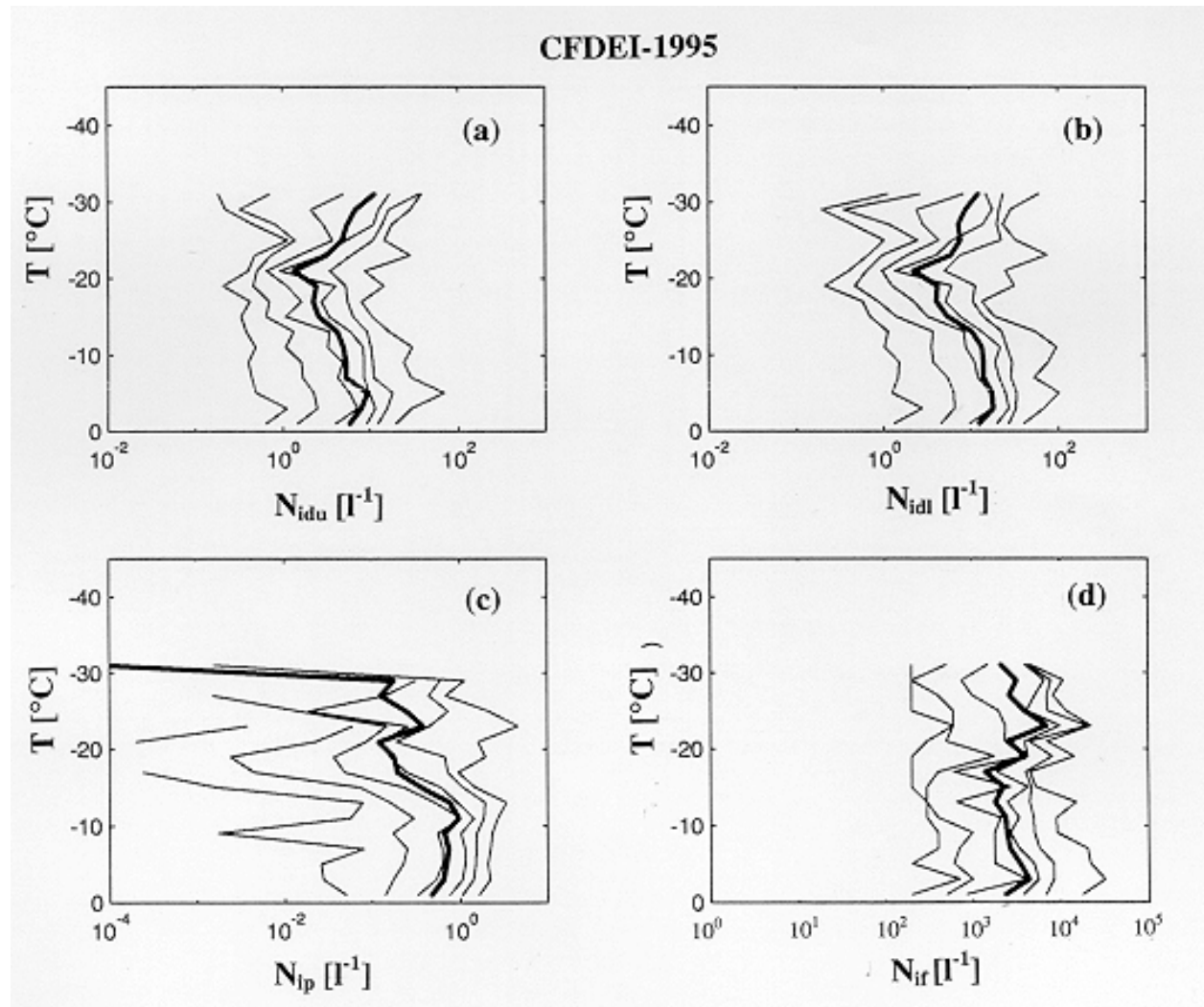


Fig. 4: Same as Fig. 3 except for CFDE I.

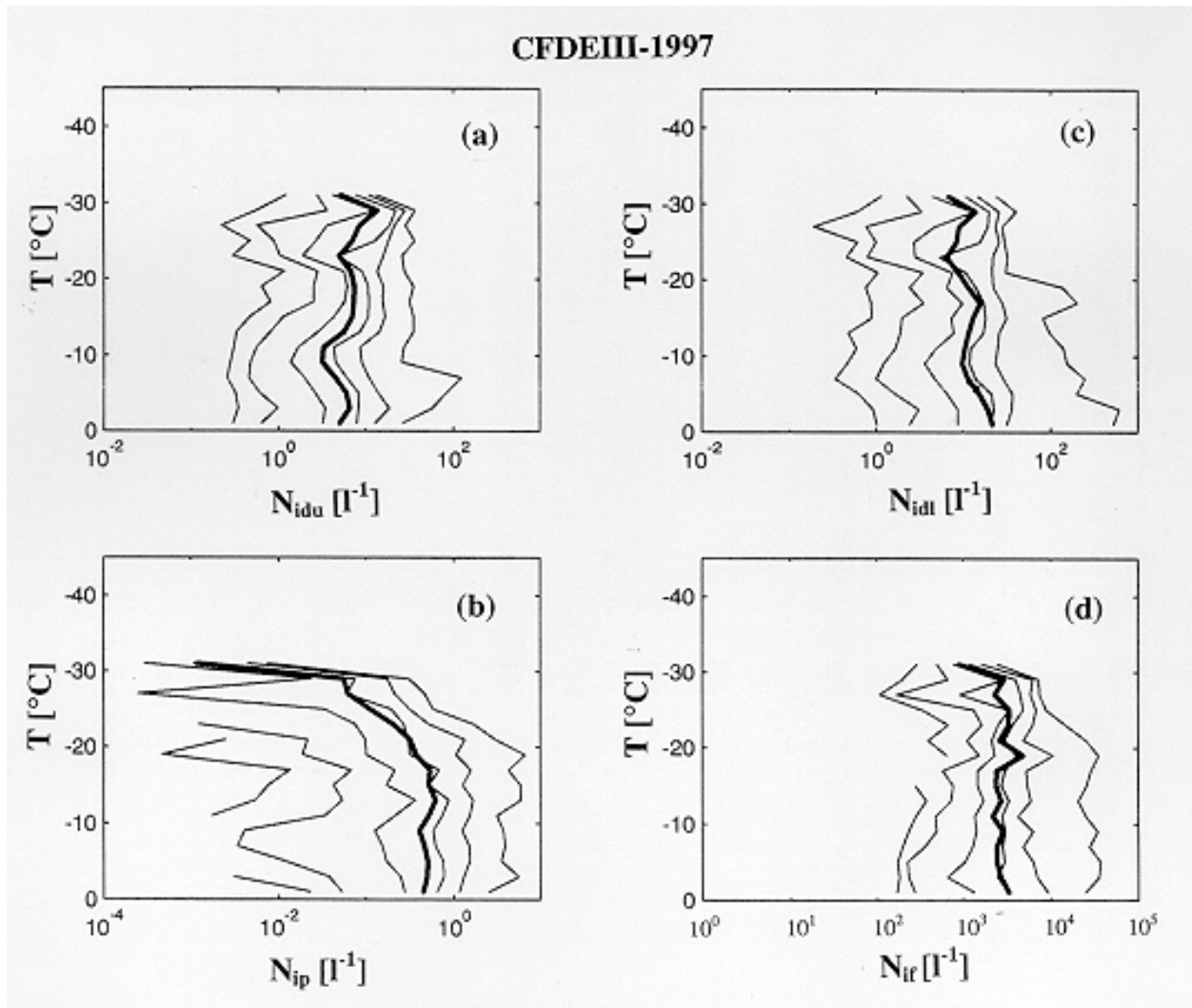


Fig. 5: Same as Fig. 3 except for CFDE III.

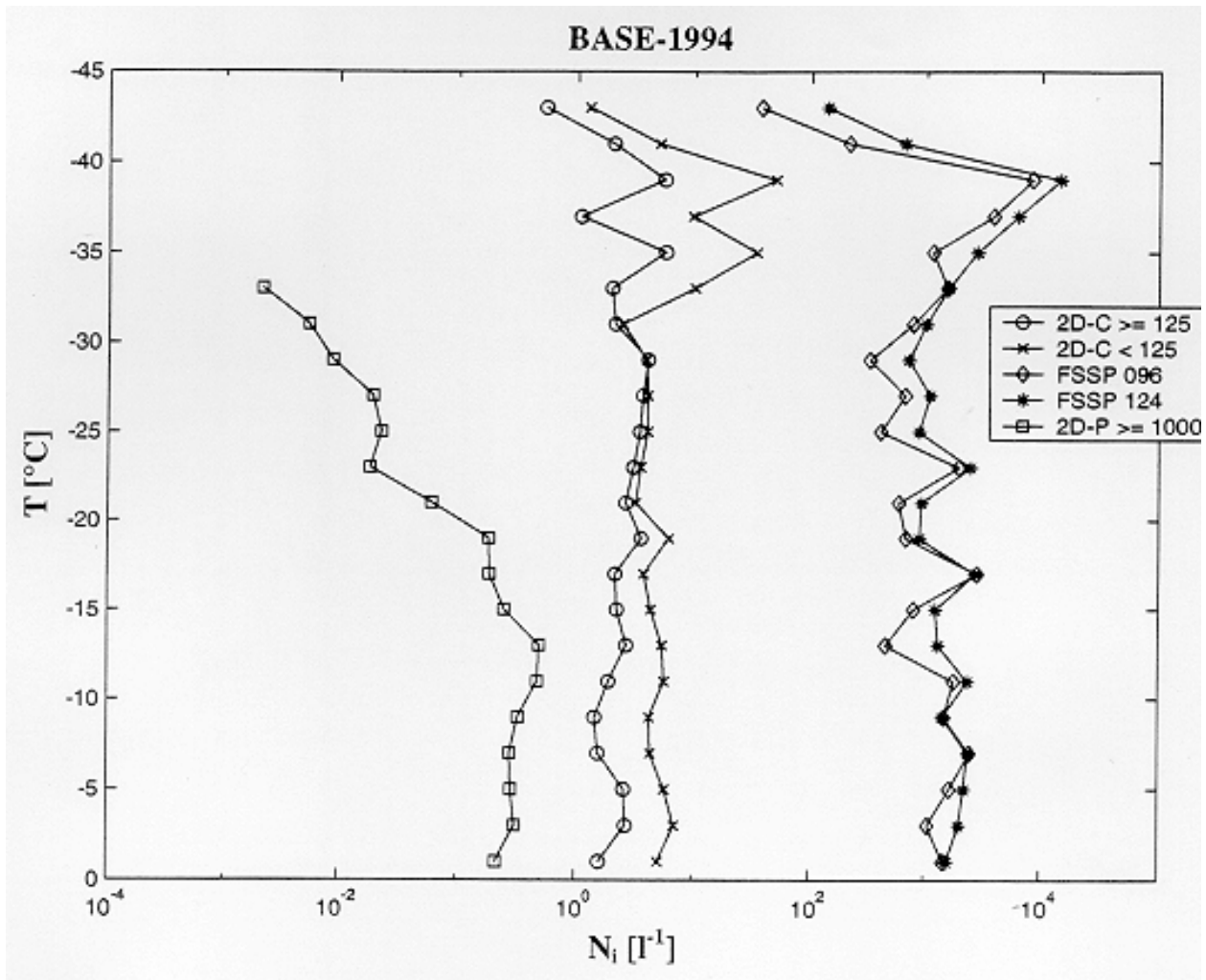


Fig. 6: The averaged N_i versus T at 2°C intervals for various probes during BASE.

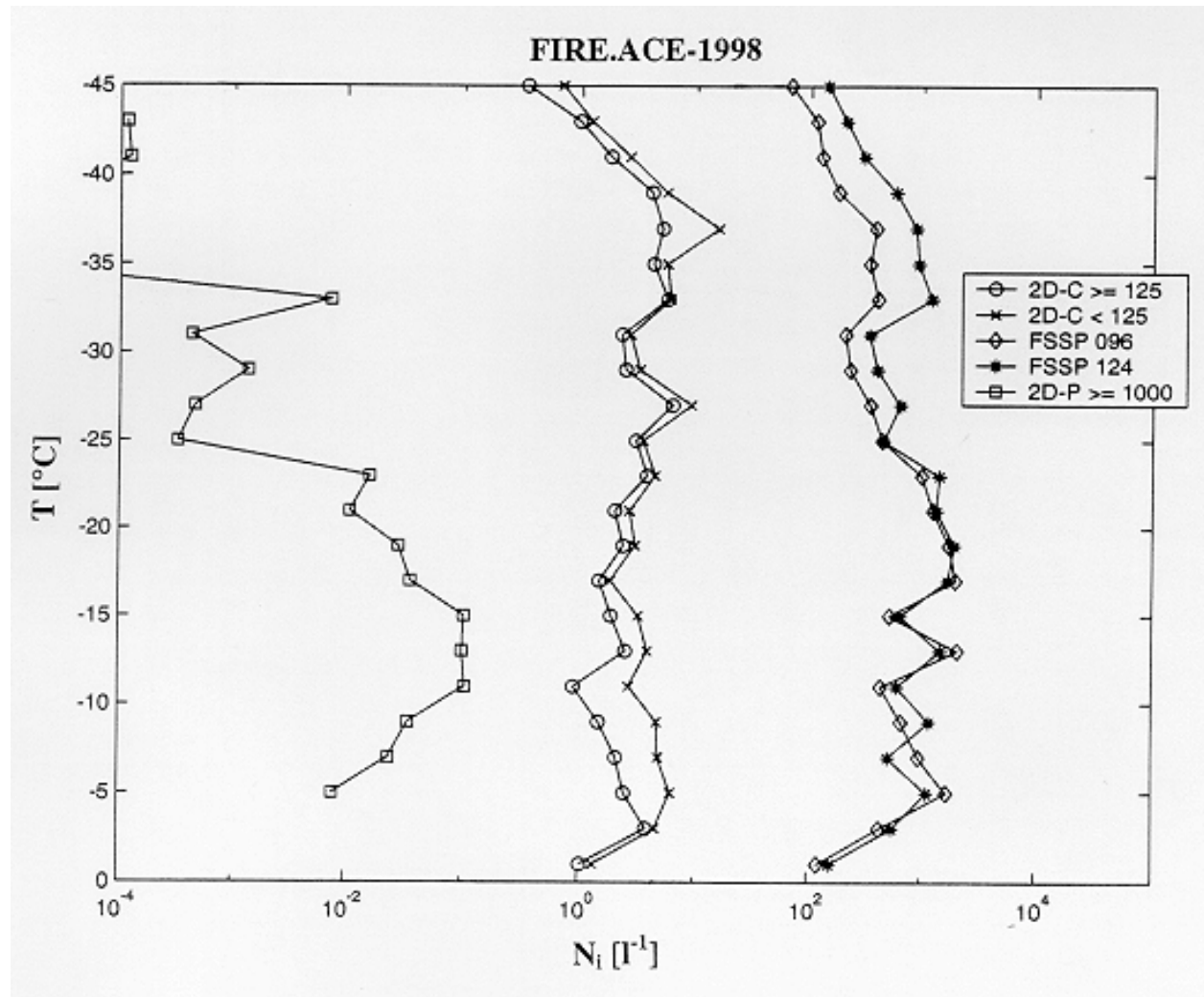


Fig. 7: The averaged N_i versus T at 2°C intervals for various probes during FIRE.ACE.

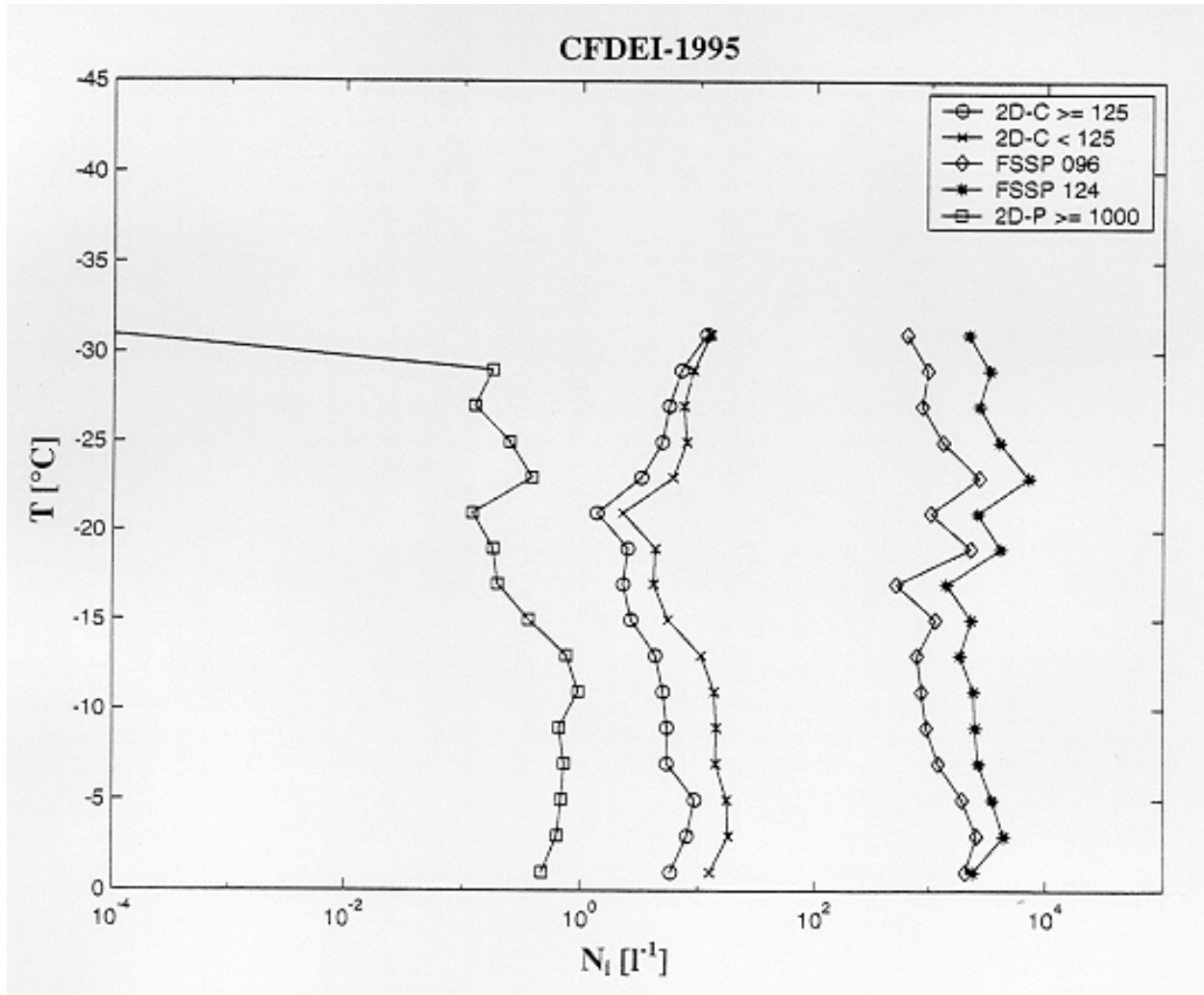


Fig. 8: The averaged N_i versus T at 2°C intervals for various probes during CFDE I.

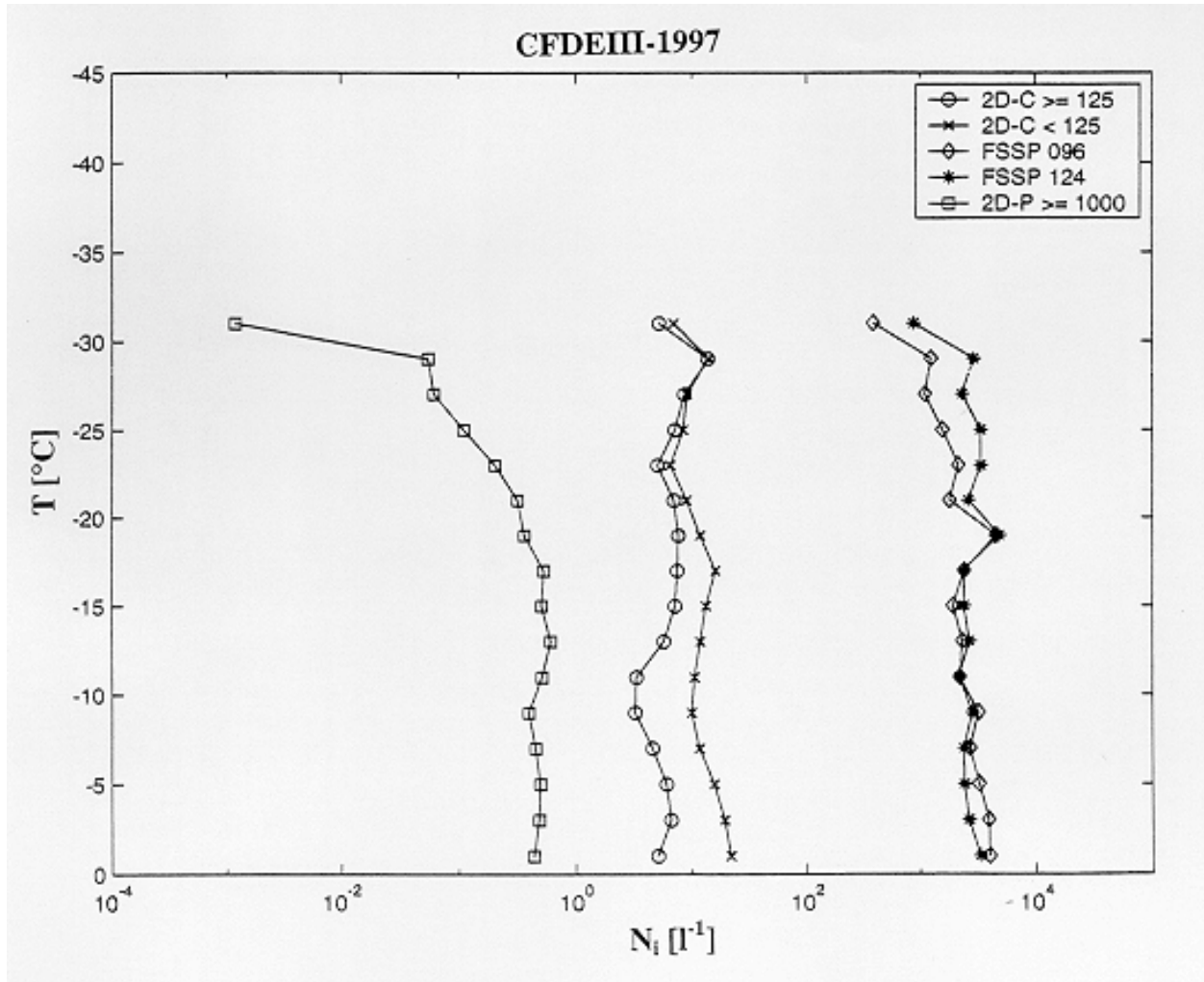


Fig. 9: The averaged N_i versus T at 2°C intervals for various probes during CFDE III.

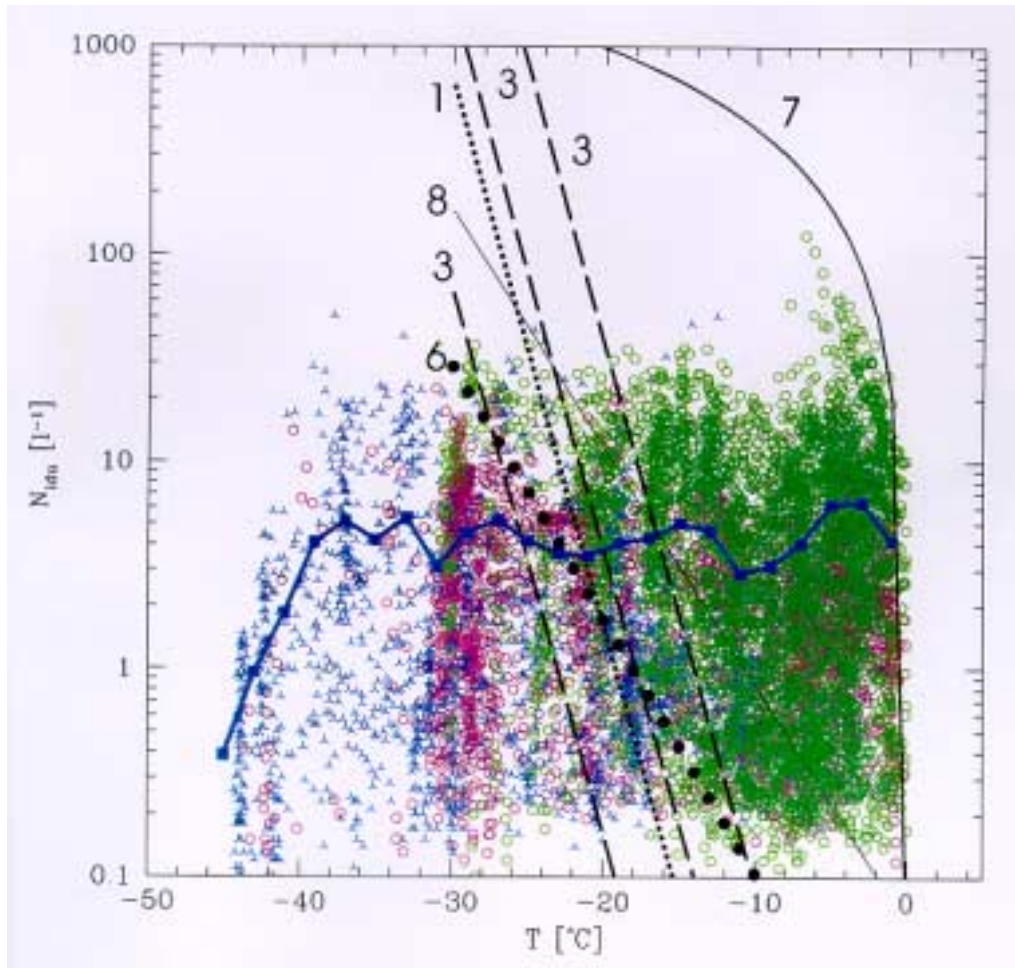


Fig. 10: The N_{idu} from 2D-C probe measurements versus T at standard conditions during BASE (open green circles), FIRE.ACE (blue triples), and CFDE (open red circles), and from the earlier studies (black lines). Note that some data points with red and blue colors are not seen because of superimposed data points. N_{idu} averaged over 2°C intervals for all projects is shown with a blue line. The thick solid line (7) is for Young (1974), dots (1) for Fletcher (1962), dashed lines (3) for Huffman and Vali (1973) assuming $S_i=0.15, 0.30, 0.45$, filled circles (6) for a fit applied to Rogers et al. (1996) observations, and the thin solid line (8) for Meyers et al. (1992). The numbers along the lines represent the parameterized equations given in Table 2. Except for Eq. (3) of Table 2, equations that are a function of S_i are not shown.

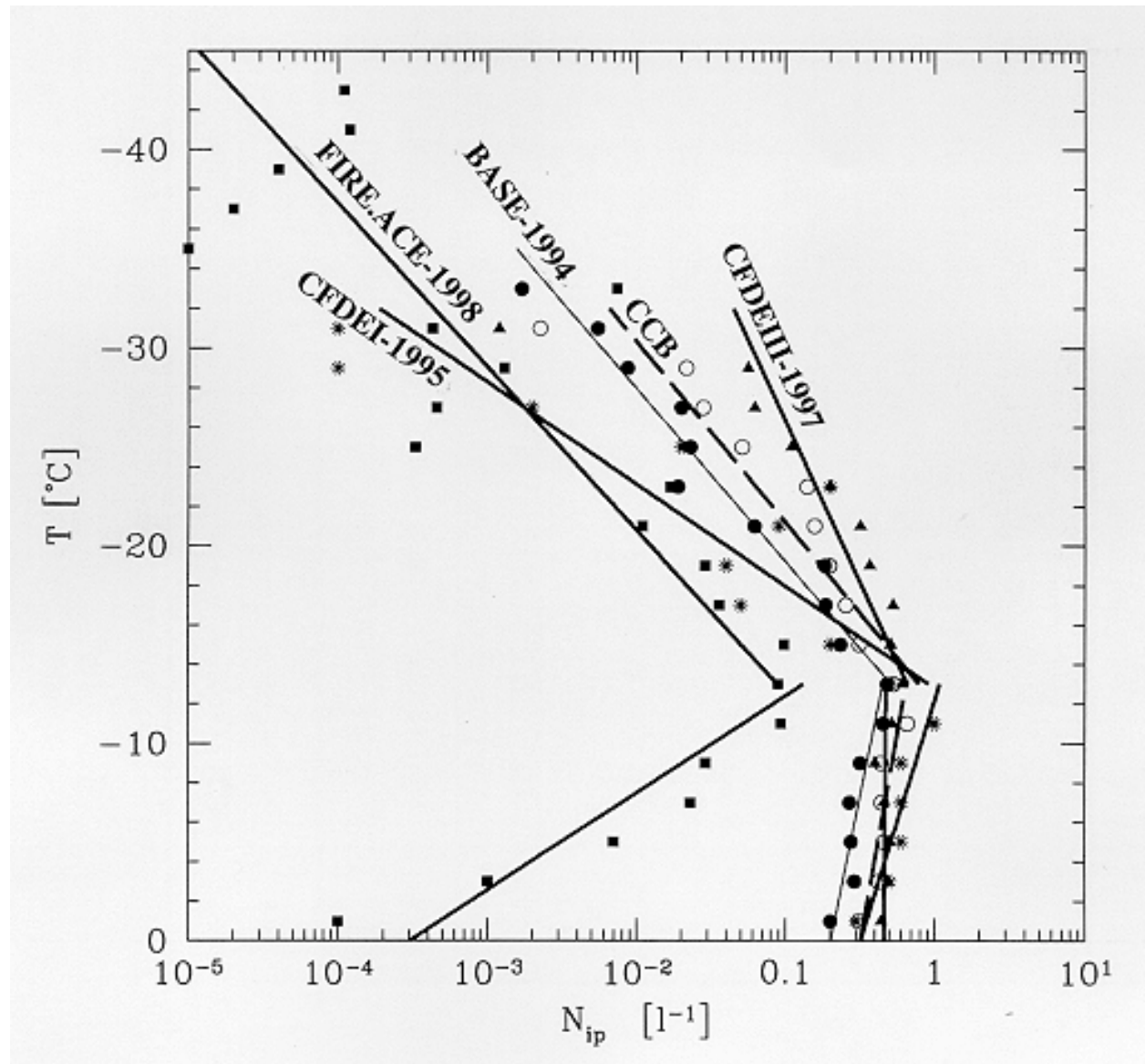


Fig. 11: The N_{ip} (size > 1000 μm) versus T over $2^{\circ}C$ intervals obtained at standard conditions: The squares, circles, triangles, and stars are for BASE, FIRE.ACE, CFDEI, and CFDEIII, respectively. The CCB line (blank circles) stands for values obtained from the CFDEI, CFDEIII, and BASE projects combined. The solid lines are for best fit and the relationships are given in Table 3. Combination of the observations from the field projects is explained in text.

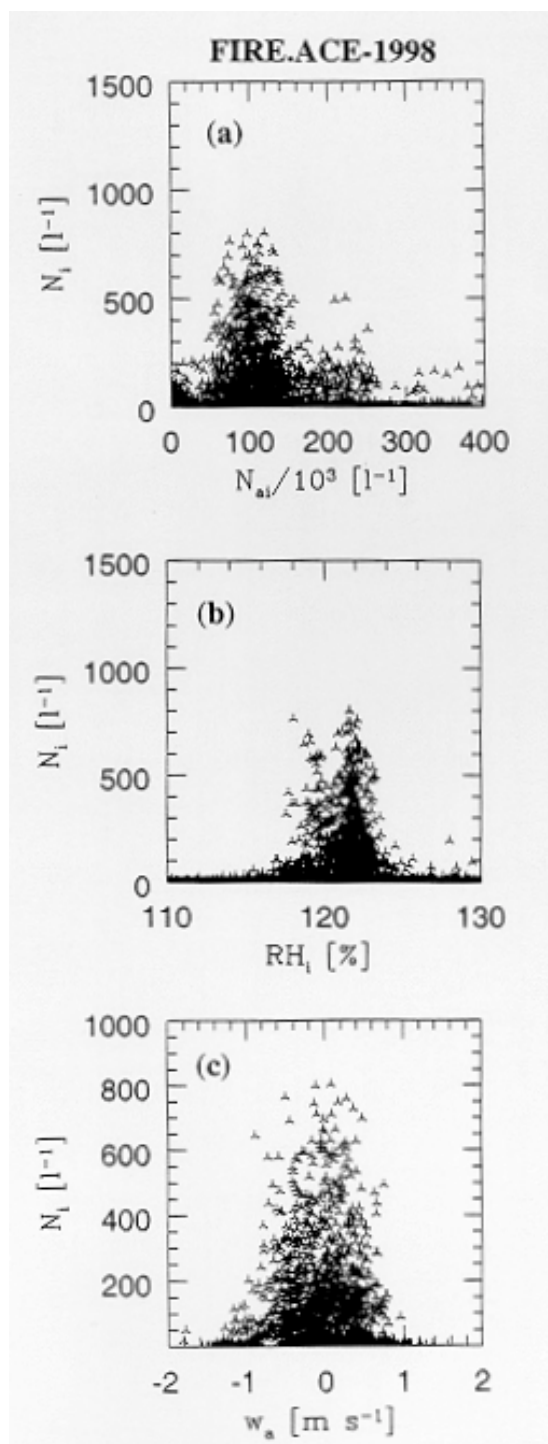


Fig. 12: N_i versus interstitial aerosol number concentration (N_{ai}) (a), N_i versus RH_i (b), and N_i versus w_a (c) for the 17 April case of FIRE.ACE. Note that N_i is the total counts from the 2D-C probe, including all particles.